

KFK-223

**KERNFORSCHUNGSZENTRUM
KARLSRUHE**

Mai 1964

KFK 223

Institut für Angewandte Reaktorphysik

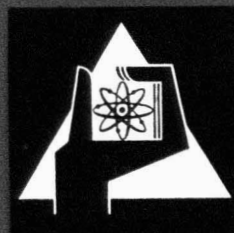
Reactor Temperature Transients with Spatial Variables

First Part: Radial Analysis

L. Calderola, E. G. Schlechtendahl

Gesellschaft für Kernforschung m.b.H.
Zentralbücherei

17.0kt



GESELLSCHAFT FÜR KERNFORSCHUNG M. B. H.

KARLSRUHE

KERNFORSCHUNGSZENTRUM KARLSRUHE

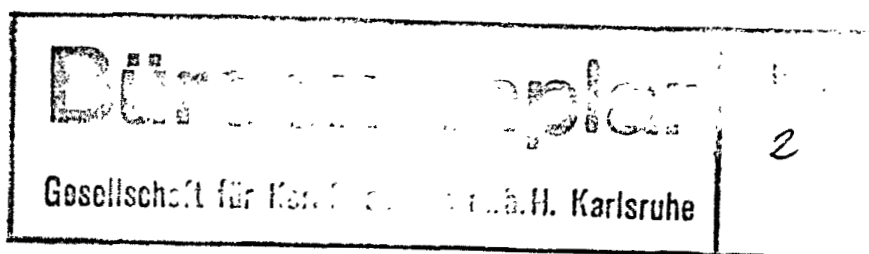
M a i 1964

K F K 223-

Institut für Angewandte Reaktorphysik

REACTOR TEMPERATURE TRANSIENTS WITH SPATIAL VARIABLES^{*)}

FIRST PART: RADIAL ANALYSIS



von

L.Caldarola^{**) und E.G.Schlechtendahl^{***)}}

Gesellschaft für Kernforschung m.b.H., Karlsruhe

^{*)}This paper has been prepared within the framework of the association Euratom - Gesellschaft für Kernforschung m.b.H. in the field of fast breeder development

<sup>**) Euratom, Brussels, delegated to the Karlsruhe Fast Reactor Project
Institute für Angewandte Reaktorphysik</sup>

^{***) Kernforschungszentrum Karlsruhe - Technische Abteilung}

Gesellschaft für Kernforschung m.b.H.

Zentralbibliothek

7. Okt. 1964

Als Manuskript vervielfältigt.

Für diesen Bericht behalten wir uns alle Rechte vor.

Gesellschaft für Kernforschung m.b.H., Karlsruhe

Contents

	<u>page</u>
1. Introduction	1
2. Mathematical Fundamentals	2
3. Expansion in sums of terms of the type $\frac{d_n}{1 + \frac{\sigma}{\sigma_n}}$	5
4. Comparison with the lumped model and physical meaning of γ	7
5. Antitransformation in sums of exponentials	9
6. Antitransformation by using for $Z(\sigma)$ the approximate expression $R(\sigma)$	10
7. Electrical Analogy and physical meaning of $Z(\sigma)$	15
8. Numerical examples	16
9. Acknowledgements	17
Appendix 1 - Solution of the heat balance equation	18
" 2 - Calculation of the average temperature variation	20
" 3 - Solution of the characteristic equation	20
" 4 - Evaluation of the coefficients associated to the series of exponentials	22
" 5 - Antitransformation by using for $Z(\sigma)$ the approximate expression $R(\sigma)$	24
Bibliography	26

Gesellschaft für Kernforschung m.b.H.
Zentralbücherei

7. Okt. 1964

List of Figures

- Fig. 1 System Geometry
- Fig. 2 Normalized zeros, $\bar{\sigma}_n$, of the characteristic equation as function of γ
- Fig. 3 Coefficients δ_{sn} associated to the poles of $G_s(\sigma)$ as function of γ
- Fig. 4 Coefficients δ_{cn} associated to the poles of $G_c(\sigma)$ as function of γ
- Fig. 5 Coefficients ε_{sn} associated to the poles of $G_{av}(\sigma) = F_s(\sigma)$ as function of γ
- Fig. 6 Coefficients ε_{cn} associated to the poles of $G_c(\sigma)$ as function of γ
- Fig. 7 Coefficients μ_n associated to the poles of $F_{av}(\sigma)$ as function of γ
- Fig. 8 Function $J_0(y \sqrt{\sigma_n})$
- Fig. 9 Polar diagram of the function $Z(\sigma)$ with $\sigma = i\nu$
- Fig. 10 Amplitude diagram of the function $Z(\sigma)$ with $\sigma = i\nu$
- Fig. 11 Phase diagram of the function $Z(\sigma)$ with $\sigma = i\nu$
- Fig. 12 Approximation of $Z(\nu)$ with $R(\nu)$
- Fig. 13 Electrical Analogy
- Fig. 14 Electrical Analogy
- Fig. 15 Polar diagrams of the functions G_s , G_{av} and G_c for $\gamma = 0.07$ with $\sigma = i\nu$
- Fig. 16 Polar diagrams of the functions F_s , F_{av} and F_c for $\gamma = 0.07$ with $\sigma = i\nu$
- Fig. 17 Approximated curves of the antitransformed of the function $\frac{1}{\sigma} F_{av}(\sigma)$ in the case $\gamma = 0.07$
- Fig. 18 Approximated curves of the antitransformed of the function $F_{av}(\sigma)$ in the case $\gamma = 0.07$
- Fig. 19 Amplitude diagram of the frequency response of $F_{av}(\sigma)$ and its approximations ($\gamma = 0.07$)
- Fig. 20 Phase diagram of the frequency response of $F_{av}(\sigma)$ and its approximations ($\gamma = 0.07$)

- Fig.21 Amplitude diagram of the frequency response of $F_s(\sigma)$ and its approximations ($\gamma = 0.07$)
- Fig.22 Phase diagram of the frequency response of $F_s(\sigma)$ and its approximations ($\gamma = 0.07$)
- Fig.23 Approximated curves of the antitransformed of the function $\frac{1}{\sigma} F_{av}(\sigma)$ in the case $\gamma = 0.35$
- Fig.24 Approximated curves of the antitransformed of the function $F_{av}(\sigma)$ in the case $\gamma = 0.35$
- Fig.25 Approximated curves of the antitransformed of the function $\frac{1}{6} F_{av}(\sigma)$ in the case $\gamma = 0.01$
- Fig.26 Approximated curves of the antitransformed of the function $F_{av}(\sigma)$ in the case $\gamma = 0.01$
- Fig.27 Graphical solution of the characteristic equation

List of Tables

Table 1 Relationship between the zeros " σ_n " and the normalized zeros " $\bar{\sigma}_n$ " of the characteristic equation

1. Introduction

In nuclear reactors the temperature transients are normally treated, by using the well known "lumped model". This model does not take into account any effect due to the heat propagation inside the fuel element and the heat transport along the channel.

Purpose of this paper is therefore a critical analysis of the solutions of the heat balance equations with spatial variables.

The work has been divided in two parts:

- (a) Radial Analysis in which the heat propagation inside the fuel element is studied
- (b) Axial Analysis: the results coming from the first part are incorporated in the heat balance equation of the coolant. Then the complete solution, including the heat transport along the channel, is analysed.

In this first part the radial analysis is developed. Two different approximate solutions have been found one expressed in sums of exponentials and the other with the error function.

Numerical examples are included with reference to Sefor reactor (Bibl.7.) and to power reactors.

For simplicity in this mathematical treatment the fuel element has been supposed to be cooled directly without any cladding. Nevertheless the method is still general if, instead of the coolant temperature, we consider the temperature of the internal surface of the cladding.

2. Mathematical Fundamentals

Fig.1 shows the section of a cylindrical fuel element in which heat is produced uniformly and which is cooled on the external surface. The following symbols have been used:

- T = temperature at any point of the cylinder
 T_s = surface temperature of the cylinder
 T_c = central temperature of the cylinder
 T_{av} = average temperature of the cylinder
 Θ = coolant temperature (or temperature of the internal surface of the cladding)
 q = power density
 r = radius
 R = external radius
 t = time
 λ = thermal conductivity (supposed to be constant)
 ρ_f = mass density (supposed to be constant)
 c_f = specific heat capacity (supposed to be constant)
 h = heat transfer coefficient between cylinder surface and coolant (supposed to be constant)

The equation which describes the heat balance in a cylinder is the following:

$$\frac{\partial T}{\partial t} = \frac{\lambda}{\rho_f c_f} \left(\frac{\partial^2 T}{\partial r^2} + \frac{1}{r} \frac{\partial T}{\partial r} \right) + \frac{q}{\rho_f c_f} \quad (1)$$

In equation (1) the term related to the heat propagation in the fuel element along the axial direction has been neglected.

The boundary conditions for the full cylinder are:

$$\int \frac{\partial T}{\partial r} \Big|_{r=0} = 0 \quad (2)$$

$$\int \frac{\partial T}{\partial r} \Big|_{r=R} = - \frac{h}{k} (T_s - \Theta) \quad (3)$$

Equation (1) can be written as follows:

$$\frac{\partial^2 T}{\partial y^2} + \frac{1}{y} \frac{\partial T}{\partial y} - \frac{\partial T}{\partial \tau} = - \frac{R}{2h\gamma} q \quad (4)$$

where:

$$y = \text{normalized radius} = \frac{r}{R} \quad (5)$$

$$\tau = \text{normalized time} = \frac{t}{t_r} \quad (6)$$

$$t_r = \frac{\rho_f c_f}{\lambda} R^2 = \text{radial time scale} \quad (7)$$

$$\gamma = \frac{\lambda}{2 h R} \quad (8)$$

Considering the variation of the system from the stationary conditions, we can introduce the following symbols:

$$\Delta T = T - T_o \quad (9)$$

$$\Delta \theta = \theta - \theta_o \quad (10)$$

$$\Delta q = q - q_o \quad (11)$$

where the subscript "o" indicates initial steady state conditions and " Δ " variation from steady state conditions.

Equation (4) becomes:

$$\frac{\partial^2 \Delta T}{\partial y^2} + \frac{1}{y} \frac{\partial \Delta T}{\partial y} - \frac{\partial \Delta T}{\partial \tau} = - \frac{R}{2 h \gamma} \Delta q \quad (12)$$

The Laplace transform of equation (12) is:

$$\frac{d^2 \Delta T^*}{dy^2} + \frac{1}{y} \frac{d \Delta T^*}{dy} - \sigma \Delta T^* = - \frac{R}{2 h \gamma} \Delta q^* \quad (13)$$

where

"*" indicates Laplace transform

σ = complex variable of the Laplace transformation

The boundary conditions (2) and (3) become respectively:

$$\left[\frac{d\Delta T^*}{dy} \right]_{y=0} = 0 \quad (14)$$

$$\left[\frac{d\Delta T^*}{dy} \right]_{y=1} = - \frac{1}{2\gamma} (\Delta T_s^* - \Delta \theta^*) \quad (15)$$

The solution of equation (13) with the associated boundary conditions (14) and (15) is the following (see Appendix 1):

$$\Delta T^* = G(\sigma; y) \Delta \theta^* + \frac{R}{2h} \left[1 + \frac{1-y^2}{4\gamma} \right] F(\sigma; y) \Delta q^* \quad (16)$$

where:

$$G(\sigma; y) = \frac{1}{1 + \frac{\gamma}{Z(\sigma)}} \frac{J_0(y\sqrt{-\sigma})}{J_0(\sqrt{-\sigma})} \quad (17)$$

$$Z(\sigma) = - \frac{J_0(\sqrt{-\sigma})}{2\sqrt{-\sigma} J_1(\sqrt{-\sigma})} \quad (18)$$

$$F(\sigma; y) = \frac{1}{1 + \frac{1-y^2}{4\gamma}} \frac{1}{\gamma \sigma} \left[1 - G(\sigma; y) \right] \quad (19)$$

$J_0(\sqrt{-\sigma})$ and $J_1(\sqrt{-\sigma})$ being Bessel functions of the first kind. For practical purposes it is useful to calculate the variation of the surface temperature, ΔT_s^* , ($y=1$), central temperature, ΔT_c^* ($y=0$), and average temperature, ΔT_{av}^* (see Appendix 2):

$$\Delta T_s^* = G_s(\sigma) \Delta \theta^* + \frac{R}{2h} F_s(\sigma) \Delta q^* \quad (20)$$

$$\Delta T_c^* = G_c(\sigma) \Delta \theta^* + \frac{R}{2h} \left[1 + \frac{1}{4\gamma} \right] F_c(\sigma) \Delta q^* \quad (21)$$

$$\Delta T_{av}^* = \frac{1}{\pi} \int_0^1 2\pi y \Delta T^* dy = G_{av}(\sigma) \Delta \theta^* + \frac{R}{2h} \left[1 + \frac{1}{8\gamma} \right] F_{av}(\sigma) \Delta q^* \quad (22)$$

in which:

$$G_s(\sigma) = \frac{1}{1 + \frac{\gamma}{Z(\sigma)}} \quad (23)$$

$$F_s(\sigma) = \frac{\frac{1}{\sigma Z(\sigma)}}{1 + \frac{\gamma}{Z(\sigma)}} = \frac{1}{\gamma \sigma} \sqrt{1 - G_s(\sigma)} \quad (24)$$

$$G_c(\sigma) = \frac{1}{1 + \frac{\gamma}{Z(\sigma)}} \quad \frac{1}{J_o(\sqrt{-\sigma})} = \frac{G_s(\sigma)}{J_o(\sqrt{-\sigma})} \quad (25)$$

$$F_c(\sigma) = \frac{1}{1 + \frac{1}{4\gamma}} \quad \frac{1}{\gamma \sigma} \sqrt{1 - G_c(\sigma)} \quad (26)$$

$$G_{av}(\sigma) = \frac{\frac{1}{\sigma Z(\sigma)}}{1 + \frac{\gamma}{Z(\sigma)}} = F_s(\sigma) \quad (27)$$

$$F_{av}(\sigma) = \frac{1}{1 + \frac{1}{8\gamma}} \quad \frac{1}{\gamma \sigma} \sqrt{1 - F_s(\sigma)} \quad (28)$$

It is very important to notice that the functions (23); (24); (27) and (28) depend only on γ and $Z(\sigma)$.

3. Expansion in sums of terms of the type $\frac{d_n}{1 + \frac{\sigma}{\sigma_n}}$

The expressions (17); (19) and (23) to (28) can be expanded in a sum of terms of the type $\frac{d_n}{1 + \frac{\sigma}{\sigma_n}}$ which in the time domain corresponds to

a sum of exponential functions.

$$G_s(\sigma) = \sum_{n=1}^{n=\infty} \frac{\delta_{sn}}{1 + \frac{\sigma}{\sigma_n}} \quad (29)$$

$$F_s(\sigma) = \sum_{n=1}^{n=\infty} \frac{\xi_{sn}}{1 + \frac{\sigma}{\sigma_n}} \quad (30)$$

$$G_c(\sigma) = \sum_{n=1}^{n=\infty} \frac{\delta_{cn}}{1 + \frac{\sigma}{\sigma_n}} \quad (31)$$

$$F_c(\sigma) = \sum_{n=1}^{n=\infty} \frac{\xi_{cn}}{1 + \frac{\sigma}{\sigma_n}} \quad (32)$$

$$G(\sigma) = \sum_{n=1}^{n=\infty} \frac{\delta_n}{1 + \frac{\sigma}{\sigma_n}} \quad (33)$$

$$F(\sigma) = \sum_{n=1}^{n=\infty} \frac{\epsilon_n}{1 + \frac{\sigma}{\sigma_n}} \quad (34)$$

$$G_{av}(\sigma) = F_s(\sigma) = \sum_{n=1}^{n=\infty} \frac{\epsilon_{sn}}{1 + \frac{\sigma}{\sigma_n}} \quad (35)$$

$$F_{av}(\sigma) = \sum_{n=1}^{n=\infty} \frac{\mu_n}{1 + \frac{\sigma}{\sigma_n}} \quad (36)$$

All the, $-\bar{\sigma}_n$, satisfy the characteristic equation:

$$1 + \frac{\gamma}{Z(\sigma)} = 0 \quad (37)$$

The roots of equation (37) are all real and negative (see Appendix 3). A graphical solution of equation (37) is shown also in Appendix 3. The equation has been solved also numerically using a digital computer IBM 7070 and values of $\bar{\sigma}_n$ up to $n=20$ have been calculated for values of γ between 10^{-4} and 10.

Fig.2 shows the normalized " $\bar{\sigma}_n$ " as function of γ . The relationship between σ_n and $\bar{\sigma}_n$ is the following:

$$\bar{\sigma}_n = b_n + (a_n - b_n) \delta_n \quad (\text{Appendix 3}) \quad (38)$$

where the meaning and the values of the coefficients a_n and b_n are given in Table 1.

The coefficients of the equations (29) to (36) are given by the following expressions (see Appendix 4):

$$\delta_{sn} = \frac{\gamma}{0.25 + \gamma^2 \sigma_n} \quad (39)$$

$$\epsilon_{sn} = \frac{1}{\sigma_n (0.25 + \gamma^2 \sigma_n)} \quad (40)$$

$$\delta_{cn} = \frac{\gamma}{0.25 + \gamma^2 \sigma_n} - \frac{1}{J_0(\sqrt{\sigma_n})} \quad (41)$$

$$\xi_{cn} = \frac{4\gamma}{1+4\gamma} \frac{1}{\sigma_n(0.25+\gamma^2\sigma_n^2)} - \frac{1}{J_0(\sqrt{\sigma_n})} \quad (42)$$

$$\delta_n = \frac{\gamma}{0.25+\gamma^2\sigma_n^2} \frac{J_0(y\sqrt{\sigma_n})}{J_0(\sqrt{\sigma_n})} \quad (43)$$

$$\xi_n = \frac{4\gamma}{4\gamma+1-y^2} \frac{1}{\sigma_n(0.25+\gamma^2\sigma_n^2)} \frac{J_0(y\sqrt{\sigma_n})}{J_0(\sqrt{\sigma_n})} \quad (44)$$

$$\mu_n = \frac{8}{1+8\gamma} \frac{1}{\sigma_n^2(0.25+\gamma^2\sigma_n^2)} \quad (45)$$

The expressions (39) to (45) satisfy the following relationships:

$$\sum_{n=1}^{n=\infty} \delta_{sn} = \sum_{n=1}^{n=\infty} \xi_{sn} = \sum_{n=1}^{n=\infty} \delta_{cn} = \sum_{n=1}^{n=\infty} \xi_{cn} = \sum_{n=1}^{n=\infty} \delta_n = \sum_{n=1}^{n=\infty} \xi_n = \sum_{n=1}^{n=\infty} \mu_n = 1 \quad (46)$$

Figs.3; 4; 5; 6; 7 show the various coefficients as function of γ .

Fig.8 shows the function $J_0(y\sqrt{\sigma_n})$.

4. Comparison with the lumped model and physical meaning of γ

The lumped model is that obtained by considering the fuel element as a simple thermal capacitance and therefore neglecting any heat propagation effect. In this case the heat balance equation is the following:

$$2\pi Rh (\Delta T - \Delta \theta) + \pi R^2 \rho_f c_f \frac{d\Delta T}{dt} = \pi R^2 \Delta q \quad (47)$$

Introducing the notations (6); (7) and (8) and making the Laplace transformation, equation (47) becomes:

$$\Delta T^* = \frac{1}{1+\gamma\sigma} \Delta \theta^* + \frac{R}{2h} \frac{1}{1+\gamma\sigma} \Delta q^* \quad (48)$$

Comparing (48) with (20), it appears that they are equal if:

$$Z(\sigma) = \frac{1}{\sigma} \quad (49)$$

The lumped model gives a good description of the transient when $\gamma \rightarrow \infty$. In fact from fig.2:

$$\lim_{\gamma \rightarrow \infty} \bar{\sigma}_1 = \frac{1}{a_1 \gamma} \quad (50)$$

and therefore:

$$\lim_{\gamma \rightarrow \infty} \sigma_1 = \frac{1}{\gamma} \quad (51)$$

and in all the expressions (29) to (36) it is:

$$\lim_{\gamma \rightarrow \infty} \delta_{sl} = \lim_{\gamma \rightarrow \infty} \epsilon_{sl} = \lim_{\gamma \rightarrow \infty} \delta_{cl} = \lim_{\gamma \rightarrow \infty} \epsilon_{cl} = \lim_{\gamma \rightarrow \infty} \delta_1 = \lim_{\gamma \rightarrow \infty} \epsilon_1 = \lim_{\gamma \rightarrow \infty} \mu_1 = 1 \quad (52)$$

and for $n \neq 1$

$$\lim_{\gamma \rightarrow \infty} \delta_{sn} = \lim_{\gamma \rightarrow \infty} \epsilon_{sn} = \lim_{\gamma \rightarrow \infty} \delta_{cn} = \lim_{\gamma \rightarrow \infty} \epsilon_{cn} = \lim_{\gamma \rightarrow \infty} \delta_n = \lim_{\gamma \rightarrow \infty} \epsilon_n = \lim_{\gamma \rightarrow \infty} \mu_n = 0 \quad (53)$$

as also it appears from figs.3 to 7.

From (20) and (21), it is possible to obtain (for $\sigma \rightarrow 0$):

$$\gamma = \frac{l}{4} \frac{T_s - \Theta}{T_c - T_s} \quad \text{with reactor in stationary conditions} \quad (54)$$

Metallic fuel elements (fig.1) are characterized by a flat temperature distribution inside the fuel element in comparison to the temperature drop between surface and coolant, that is $T_c - T_s \ll T_s - \Theta$ (γ big). Their temperature transients are therefore well described by the lumped model.

In the case of ceramic fuel elements (as in Sefor) the temperature distribution inside the fuel element is very shaped ($T_c - T_s \gg T_s - \Theta$; γ small) and therefore the more refined model is needed to describe the temperature transients.

γ has also other two physical meanings:

$$\gamma = \frac{\lambda}{2hR} = \frac{1}{4} \frac{l/2\pi Rh}{l/4\pi\lambda} = \frac{1}{4} \frac{\text{thermal resistance between fuel and coolant}}{\text{equivalent thermal resistance of the fuel}} \quad (54')$$

with heat production supposed to be concentrated in the center of the fuel element, and

$$\gamma = \frac{\rho_f c_f R^2 h}{\rho_f c_f R^2 / \lambda} = \frac{t_1}{t_r} = \frac{\text{time constant of the lumped model}}{\text{radial time scale}} \quad (54'')$$

5. Antitransformation in sums of exponentials

All the transfer functions calculated in paragraph 3 are of the type:

$$M(\sigma) = \sum_{n=1}^{n=\infty} \frac{d_n}{1 + \frac{\sigma}{\sigma_n}} \quad (55)$$

with:

$$\sigma_{n+1} > \sigma_n \quad (56)$$

$$\left| d_{n+1} \right| < \left| d_n \right| \quad (57)$$

$$\sum_{n=1}^{n=\infty} d_n = 1 \quad (58)$$

Let us consider the case in which the power (or the coolant temperature) is a step function. In this case an expression of the type

$$X^*(\sigma) = \frac{1}{\sigma} \sum_{n=1}^{n=\infty} \frac{d_n}{1 + \frac{\sigma}{\sigma_n}} \quad (59)$$

must be antitransformed. The solution in the time domain is:

$$X(\tau) = 1 - \sum_{n=1}^{n=\infty} d_n e^{-\sigma_n \tau} \quad (60)$$

For practical purposes the series of exponentials must be arrested to a value $n=m$. We shall consider the two approximate solutions:

$$X_{m+}(\tau) = 1 - \sum_{n=1}^{n=m} d_n e^{-\sigma_n \tau} \quad (\text{upper approximation}) \quad (61)$$

$$X_{m-}(\tau) = 1 - \sum_{n=1}^{n=m} d_n e^{-\sigma_n \tau} \quad (\text{lower approximation}) \quad (62)$$

where:

$$\frac{1}{D_m} = \sum_{n=1}^{n=m} d_n < 1 \quad (63)$$

At any value of γ it is:

$$X_{m-}(\gamma) < X(\gamma) < X_{m+}(\gamma) \quad (64)$$

The transfer functions corresponding to equations (61) and (62) are respectively:

$$M_+(\sigma) = \sigma X_{m+}^*(\sigma) = \left(1 - \frac{1}{D_m} + \sum_{n=1}^{n=m} \frac{d_n}{1 + \frac{\sigma}{\sigma_n}} \right) \quad (65)$$

$$M_-(\sigma) = \sigma X_{m-}^*(\sigma) = D_m \sum_{n=1}^{n=m} \frac{d_n}{1 + \frac{\sigma}{\sigma_n}} \quad (66)$$

6. Antittransformation by using for $Z(\sigma)$ the approximate expression $R(\sigma)$

The mathematical treatment already described gives rapidly convergent approximated expressions for the functions $F_s(\sigma)$, $F_c(\sigma)$ and $F_{av}(\sigma)$.

In the case of $G_s(\sigma)$ the approximated expressions are not rapidly convergent for small values of γ .

A complete different approach to the problem is to make the antittransformation by direct integration along the imaginary axis of the complex plane.

Let us examin the frequency response of the function $Z(\sigma)$, that is when $\sigma = i\nu$

$$Z(\nu) = e^{-\frac{\pi}{4}i} \frac{J_0(e^{\frac{3\pi}{4}i}\sqrt{\nu})}{2\sqrt{\nu} J_1(e^{\frac{3\pi}{4}i}\sqrt{\nu})} \quad (67)$$

Fig.9 shows the polar diagram of $Z(\nu)$ and figs.10 and 11 amplitude and phase of $Z(\nu)$ as function of ν .

From the asymptotic expressions of the Bessel functions, it is possible to calculate:

$$\lim_{\nu \rightarrow 0} Z(\nu) = \frac{1}{8} + \frac{1}{i\nu} \quad (68)$$

$$\lim_{\nu \rightarrow \infty} Z(\nu) = \frac{1}{2\sqrt{i\nu - 1}} \quad (69)$$

Let us consider the function:

$$R(\nu) = \frac{\sqrt{1+0.25 i\nu}}{i\nu} \quad (\text{Bibl.3}) \quad (70)$$

which has the asymptotes:

$$\lim_{\nu \rightarrow 0} R(\nu) = \frac{1}{8} + \frac{1}{i\nu} \quad (71)$$

$$\lim_{\nu \rightarrow \infty} R(\nu) = \frac{1}{2\sqrt{i\nu}} \quad (72)$$

Fig.12 shows the errors in amplitude and phase made by substituting $Z(\nu)$ with $R(\nu)$.

Putting $R(\sigma)$ in the expressions $G_s(\sigma)$; $F_s(\sigma)$ and $F_{av}(\sigma)$, we obtain:

$$G_s(\sigma) \approx \frac{\sqrt{1+0.25\sigma}}{\sqrt{1+0.25\sigma} + \gamma\sigma} \quad \text{when } \sigma = i\nu \quad (73)$$

$$F_s(\sigma) \approx \frac{1}{\gamma\sigma + \sqrt{1+0.25\sigma}} \quad \text{when } \sigma = i\nu \quad (74)$$

$$F_{av}(\sigma) \approx \frac{1}{1 + \frac{1}{8\gamma}} \quad \frac{1}{\gamma\sigma} \quad \frac{\gamma\sigma + \sqrt{1+0.25\sigma} - 1}{\gamma\sigma + \sqrt{1+0.25\sigma}} \quad \text{when } \sigma = i\nu \quad (75)$$

Let us consider now the case in which the power (or the coolant temperature) is a step function. Then the antitransformed are:

$$L^{-1} \left[\frac{1}{\sigma} G_s(\sigma) \right] \approx 1(T) - \frac{\beta-\alpha}{2\beta} e^{-\frac{(\beta-\alpha)}{\gamma} T} \left[1 + E \left[2(\beta-\alpha)\sqrt{T} \right] \right] - \\ - \frac{\beta+\alpha}{2\beta} e^{\frac{\alpha+\beta}{\gamma} T} \left[1 - E \left[2(\beta+\alpha)\sqrt{T} \right] \right] \quad (76)$$

$$L^{-1} \left[\frac{1}{\sigma} F_s(\sigma) \right] \approx E(2\sqrt{\gamma}) - \frac{1}{2\beta} e^{-\frac{\beta-\alpha}{\gamma} T} \left[1 + E \left[2(\beta-\alpha)\sqrt{T} \right] \right] + \\ + \frac{1}{2\beta} e^{\frac{\alpha+\beta}{\gamma} T} \left[1 - E \left[2(\beta+\alpha)\sqrt{T} \right] \right] \quad (77)$$

$$L^{-1} \left[\frac{1}{\sigma} F_{av}(\sigma) \right] \equiv \frac{8\gamma}{1+8\gamma} \left\{ \cdot 1(T) + \frac{E(2\sqrt{\gamma})}{8\gamma} - \frac{\sqrt{\gamma} e^{-4T}}{\gamma \cdot 2\sqrt{\pi}} \right. \\ \left. + \frac{T}{\gamma} \left[1 - E(2\sqrt{\gamma}) \right] - \frac{\beta+\alpha}{2\beta} e^{-\frac{\beta-\alpha}{\gamma} T} \left[1 + E \left[2(\beta-\alpha)\sqrt{T} \right] \right] - \right. \\ \left. - \frac{\beta-\alpha}{2\beta} e^{\frac{\alpha+\beta}{\gamma} T} \left[1 - E \left[2(\beta+\alpha)\sqrt{T} \right] \right] \right\} \quad (78)$$

where:

L^{-1} = antittransformation

E = error function

$\alpha = \frac{0.125}{\gamma}$ (79)

$\beta = \sqrt{1+\alpha^2}$ (80)

(77) and (78) can be obtained directly by (74) and (75) or by (76), taking into account (24) and (28).

Using (24) and (28), it is also possible to evaluate the case in which the power is a pulse function.

In fact:

$$L^{-1}[F_s(\sigma)] = L^{-1}\left[\frac{1}{\gamma\sigma} - \frac{1}{\gamma\sigma}G_s(\sigma)\right] = \frac{1}{\gamma} \left[1(\tau) - L^{-1}\left[\frac{1}{\sigma}G_s(\sigma)\right]\right] \quad (81)$$

and

$$L^{-1}[F_{av}(\sigma)] = \frac{1}{1 + \frac{1}{8\gamma}} L^{-1}\left[\frac{1}{\gamma\sigma} - \frac{1}{\gamma\sigma}F_s(\sigma)\right] = \frac{8}{1+8\gamma} \left[1(\tau) - L^{-1}\left[\frac{1}{\sigma}F_s(\sigma)\right]\right] \quad (82)$$

where $L^{-1}\left[\frac{1}{\sigma}G_s(\sigma)\right]$ and $L^{-1}\left[\frac{1}{\sigma}F_s(\sigma)\right]$ are already given respectively by (77) and (78).

It is possible to demonstrate that for $\gamma \rightarrow \infty$ the expressions (76); (77) and (78) all tend to:

$$1 - e^{-\frac{\tau}{\gamma}} \quad , \quad (83)$$

which is the solution given by the lumped model.

It is very interesting to examin the behaviour of the expression (76) for $\gamma \rightarrow 0$. It is:

$$\lim_{\gamma \rightarrow 0} L^{-1}\left[\frac{1}{\sigma}G_s(\sigma)\right] = 1(\tau) - 16\gamma^2 e^{-4\tau} \left[1+E(8\sqrt{\tau})\right] - e^{\tau/4\gamma^2} \left[1-E\left(\frac{\sqrt{\tau}}{2\gamma}\right)\right] \rightarrow 1(\tau) \quad (84)$$

which is difficult to approximate with expressions like (59). Instead from (77) and (78):

$$\lim_{\gamma \rightarrow 0} L^{-1}\left[\frac{1}{\sigma}F_s(\sigma)\right] = E(2\sqrt{\tau}) \quad (85)$$

$$\lim_{\gamma \rightarrow 0} L^{-1}\left[\frac{1}{\sigma}F_{av}(\sigma)\right] = E(2\sqrt{\tau}) + 8\tau \left[1-E(2\sqrt{\tau})\right] + \frac{4}{\sqrt{\pi}}\sqrt{\tau}e^{-4\tau} \quad (86)$$

which can be easier approximated by espressions like (59). This explains why the series of d_{sn} (fig.3) is poorly convergent for small values of γ , while the series of ξ_{sn} and μ_n (figs.5 and 7) are rapidly convergent. (76); (77) and (78) can be developed in expressions of the type:

$$\sum_{n=1}^{n=\infty} d_n (\sqrt{\tau})^n \quad (87)$$

where the "d_n" are functions of γ .

For $T \rightarrow 0$, we have:

$$\lim_{T \rightarrow 0} L^{-1}\left[\frac{1}{\sigma} G_s(\sigma)\right] = \frac{\sqrt{T}}{\gamma \sqrt{\pi}} - \frac{T}{4\gamma^2} \dots \quad (88)$$

$$\lim_{T \rightarrow 0} L^{-1}\left[\frac{1}{\sigma} F_s(\sigma)\right] = \frac{T}{\gamma} - \frac{2(\sqrt{T})^3}{3\gamma^2 \sqrt{\pi}} + \frac{T^2}{8\gamma^3} \dots \quad (89)$$

$$\lim_{T \rightarrow 0} L^{-1}\left[\frac{1}{\sigma} F_{av}(\sigma)\right] = \frac{8}{1+8\gamma} \left[T - \frac{T^2}{2\gamma} + \frac{4(\sqrt{T})^5}{15\gamma^2 \sqrt{\pi}} - \frac{T^3}{24\gamma^3} \dots \right] \quad (90)$$

Let us consider the case in which the coolant temperature remain constant and the power changes as a pulse function $H \cdot \delta(T)$, H being the energy of the pulse. From (22) and (82), we have:

$$\frac{2h}{R} \frac{8\gamma}{1+8\gamma} \frac{\Delta T_{av}(T)}{H/V_f} = L^{-1}[F_{av}(\sigma)] = \frac{8}{1+8\gamma} \left[l(T) - L^{-1}\left[\frac{1}{\sigma} F_s(\sigma)\right] \right] \quad (91)$$

V_f being the volume of fuel in reactor.

For $T \rightarrow 0$, (91) becomes:

$$\frac{2h}{R} \frac{8\gamma}{1+8\gamma} \frac{\Delta T_{av}(T)}{H/V_f} \rightarrow \frac{8}{1+8\gamma} \left[l(T) - \frac{T}{\gamma} + \frac{2(\sqrt{T})^3}{3\gamma^2 \sqrt{\pi}} \dots \right] \quad (92)$$

In the region $0 < T \ll \gamma$ the temperature change is a step function which is the integral of the pulse. In this interval the temperature change can be considered proportional to the time integral of the power change, which means that all the heat produced remains inside the fuel rod.

In a super-prompt critical reactivity ramp test (Bibl.6) the power changes in a way very similar to a pulse function, so that we can suppose that all the heat produced remains inside the fuel rods as long as:

$$T_{max} \ll \gamma$$

In the real time domain, taking into account (54''), condition (93) becomes:

$$t_{max} \ll \gamma t_r = \frac{\rho_f c_f R}{2h} = t_\ell = \text{time constant of the lumped model} \quad (94)$$

In order to increase the useful experiment time, t_{\max} , reactors like Sefor, designed specifically for this type of experiment, must have fuel rods with big radius.

In the Sefor case, it is:

$$\gamma = 0.07 \quad (95)$$

$$t_r = 160 \text{ secs.} \quad (96)$$

$$t_f = 11.2 \text{ secs.} \quad (97)$$

7. Electrical Analogy and physical meaning of $Z(\sigma)$

Fig.13 A shows the cylindrical electrical line equivalent to eq.(1): temperatures are represented by voltages, heat flows by currents, heat sources by current sources, heat resistances by electrical resistances and heat capacitances by electrical capacitances.

Fig.13 B shows the same cylindrical electrical line having introduced the normalized time, T , the normalized radius, y , and γ . This line is equivalent to eq.(13). The functions $G_s(\sigma)$; $F_s(\sigma)$; $G_c(\sigma)$; $F_c(\sigma)$; $G_{av}(\sigma)$ and $F_{av}(\sigma)$ can therefore be calculated by solving the electrical network of fig.13 B. If in fig.13 B we put $\Delta q = 0$, we can calculate $G_s(\sigma)$. Applying the usual network theorems, we can get the simple circuit of fig.14 A in which $Z(\sigma)$ is the output impedance of the cylindrical electrical line.

An empirical approach to calculate temperature transients in a cylindrical fuel element is usually the following: to divide the fuel element in "n" concentric cylinders having the same thickness and to write for each cylinder the equation of the lumped model. This leads to solve the electrical network of fig.14 B. From this network we can calculate approximate expressions for $G_s(\sigma)$; $F_s(\sigma)$; $G_c(\sigma)$; $F_c(\sigma)$; $G_{av}(\sigma)$ and $F_{av}(\sigma)$ and by comparison with the exact functions (23); (24); (25); (26); (27) and (28), it is possible to establish for any function how many concentric cylinders are needed in order to get the wanted degree of accuracy. In the case of $G_s(\sigma)$; $F_s(\sigma)$; $G_{av}(\sigma)$ and $F_{av}(\sigma)$, since they depend only on γ and on $Z(\sigma)$, the problem is reduced to calculate the

output impedance $Z(\sigma)$ of the electrical network of fig.14 B:

$$Z(\sigma) = \frac{1}{\sigma \frac{2n-1}{n^2} + \frac{1}{\frac{1}{2n-1} + \frac{1}{\sigma \frac{2n-3}{n^2} + \frac{1}{\frac{1}{2n-3} + \dots}}}} \quad (98)$$

8. Numerical Examples

Fig.15 shows the polar diagram of the functions $G_s(i\nu)$; $G_c(i\nu)$ and $G_{av}(i\nu)$ in the Sefor case ($\gamma=0.07$). Fig.16 shows the polar diagram of the functions $F_s(i\nu)$; $F_c(i\nu)$ and $F_{av}(i\nu)$ always in the Sefor case. In both the figures the dotted line represents the lumped model. The value $\gamma=0.07$ has been calculated including in "h" the heat transfer coefficients fuel to cladding, internal to external surface of the cladding and cladding to coolant. Let us consider the average temperature transients in the two simple cases in which the power, P , changes as a step $[\Delta P_o \cdot l(\tau)]$ and as a pulse function $[H \cdot \delta(\tau)]$, H being the energy of the pulse. During the transients under consideration, it has been supposed that the coolant temperature, Θ , is constant.

We have from (22) in the case of the step function:

$$\Delta T_{av}(\tau) = \frac{R \cdot \Delta q_o}{2h} \left[1 + \frac{1}{8\gamma} \right] L^{-1} \left[\frac{1}{\sigma} F_{av}(\sigma) \right] = \frac{R}{2h} \frac{\Delta P_o}{V_f} \frac{8\gamma}{1+8\gamma} \left[\frac{1}{\sigma} F_{av}(\sigma) \right] \quad (99)$$

V_f being the volume of fuel in reactor.

From (22) and (28) in the case of the pulse function we have:

$$\Delta T_{av}(\tau) = \frac{RH}{2h V_f} \left[1 + \frac{1}{8\gamma} \right] L^{-1} [F_{av}(\sigma)] = \frac{RH}{2h V_f} \frac{1}{\gamma} L^{-1} \left[\frac{1}{\sigma} - \frac{1}{\sigma} F_s(\sigma) \right] \quad (100)$$

Fig.17 shows the function $\frac{2hV_f}{R\Delta P_o} \frac{1}{1 + \frac{1}{8\gamma}} \Delta T_{av}(\tau) = L^{-1} \left[\frac{1}{\sigma} F_{av}(\sigma) \right]$.

Fig.18 shows the function $\frac{2hV_f}{RH} \frac{1}{1 + \frac{1}{8\gamma}} \Delta T_{av}(\tau) = L^{-1} [F_{av}(\sigma)]$.

Both the figures are referred to the Sefor case ($\gamma=0.07$). Both the figures have on the horizontal axis the normalized time scale and the real time scale. The vertical axis of fig.17 has the scale relative to $L^{-1} \left[\frac{1}{6} F_{av}(\delta) \right]$ and that relative to $\Delta T_{av}/\Delta P$ in $^{\circ}\text{C}/\text{MW}$. The vertical axis of fig.18 has the scale relative to $L^{-1} [F_{av}(\delta)]$ and that relative to $\Delta T_{av}/H$ in $^{\circ}\text{C}/\text{MW sec.}$

Fig.21 and 22 show respectively amplitude and phase of the frequency response of the function $\frac{1}{6} F_s(\delta)$ and its approximations which enter in (100).

The upper and lower approximations with exponentials have been calculated according to (65) and (66). The frequency response is better approximated by increasing the number "n" of exponentials (fig.21 and 22).

Fig.23 and 24 show the case $\gamma=0.35$ and figs.25 and 26 the case $\gamma=0.01$. These two values of γ have been chosen as limiting values of the range in which γ can vary depending on the uncertainty of the heat transfer characteristics of a power reactor. Particularly the heat transfer constant "h" can have very different values depending mainly on the model used to calculate the heat transfer coefficient fuel to cladding (gap conduction or contact conductance model)

9. Acknowledgements

The authors wish to thank Dr.W.Häfele who had with them discussions which were very useful to the preparation of this paper.

The authors thank also Miss. Ferranti who programmed and carried out the necessary calculations with the IBM 7070 computer.

Appendix 1 - Solution of the heat balance equation

The Laplace transform of the heat balance equation is (eq.13 of par.2):

$$\frac{d^2 \Delta T^*}{dy^2} + \frac{1}{y} \frac{d\Delta T^*}{dy} - \sigma \Delta T^* = - \frac{R}{2h\gamma} \Delta q^* \quad (1)$$

and the boundary conditions are (eqs.14 and 15 of par.2):

$$\left[\frac{d\Delta T^*}{dy} \right]_{y=0} = 0 \quad (2)$$

$$\left[\frac{d\Delta T^*}{dy} \right]_{y=1} = - \frac{1}{2\gamma} (\Delta T_s^* - \Delta \theta^*) \quad (3)$$

$$\text{with } \gamma = \frac{\lambda}{2hR} \quad (4)$$

The solution of equation (1) is:

$$\Delta T^* = \frac{R}{2h\gamma\sigma} \Delta q^* + A J_0(y\sqrt{-\sigma}) + B K_0(y\sqrt{-\sigma}) \quad (5)$$

where the symbols J and K indicate Bessel functions respectively of first and second kind.

Boundary condition (2) gives:

$$B = 0 \quad (6)$$

and therefore (5) becomes

$$\Delta T^* = \frac{R}{2h\gamma\sigma} \Delta q^* + A J_0(y\sqrt{-\sigma}) \quad (7)$$

Differentiating equation (7), we obtain:

$$\frac{d(\Delta T^* - \frac{R}{2h\gamma\sigma} \Delta q^*)}{dy} = - A \sqrt{-\sigma} J_1(y\sqrt{-\sigma}) \quad (8)$$

The ratio between (7) and (8) gives:

$$\frac{\Delta T^* - \frac{R}{2h\gamma\sigma} \Delta q^*}{\frac{d(\Delta T^* - \frac{R}{2h\gamma\sigma} \Delta q^*)}{dy}} = 2y Z(y^2\sigma) \quad (9)$$

where:

$$Z(y^2\sigma) = - \frac{J_0(y\sqrt{-\sigma})}{2y\sqrt{-\sigma} J_1(y\sqrt{-\sigma})} \quad (10)$$

Taking into account (9), (3) becomes:

$$\frac{1}{2Z(\sigma)} \left[\Delta T_s^* - \frac{R}{2h\gamma\sigma} \Delta q^* \right] = - \frac{1}{2\gamma} (\Delta T_s^* - \Delta \theta^*) \quad (11)$$

and therefore:

$$\Delta T_s^* = G_s(\sigma) \Delta \theta^* + \frac{R}{2h} F_s(\sigma) \Delta q^* \quad (12)$$

where:

$$G_s(\sigma) = \frac{1}{1 + \frac{\gamma}{Z(\sigma)}} \quad (13)$$

and

$$F_s(\sigma) = \frac{\frac{1}{\sigma Z(\sigma)}}{1 + \frac{\gamma}{Z(\sigma)}} = \frac{1}{\gamma\sigma} \left[1 - G_s(\sigma) \right] \quad (14)$$

From (7) and (12), we obtain (putting $y = 1$):

$$A = \frac{G_s(\sigma)}{J_0(\sqrt{-\sigma})} \Delta \theta^* - \frac{R}{2h} \frac{1}{\gamma\sigma} \frac{G_s(\sigma)}{J_0(\sqrt{-\sigma})} \Delta q^* \quad (15)$$

Introducing (15) in (7), we have:

$$\Delta T^* = G(y; \sigma) \Delta \theta^* + \frac{R}{2h} \left[1 + \frac{1-y^2}{4\gamma} \right] F(y; \sigma) \Delta q^* \quad (16)$$

where:

$$G(y; \sigma) = G_s(\sigma) \frac{J_0(y\sqrt{-\sigma})}{J_0(\sqrt{-\sigma})} = \frac{1}{1 + \frac{\gamma}{Z(\sigma)}} \frac{J_0(y\sqrt{-\sigma})}{J_0(\sqrt{-\sigma})} \quad (17)$$

and

$$F(y; \sigma) = \frac{1}{1 + \frac{1-y^2}{4\gamma}} \frac{1}{\gamma\sigma} \left[1 - G(y; \sigma) \right] \quad (18)$$

Appendix 2 - Calculation of the average temperature variation

The average temperature is given by the following formula:

$$\Delta T_{av}^* = \frac{1}{\pi} \int_0^1 2\pi y \Delta T^* dy \quad (1)$$

Taking into account equations (17) and (18) of Appendix 1, we can write:

$$\Delta T_{av} = G_{av}(\sigma) \Delta \theta^* + \frac{R}{2h} \left(1 + \frac{1}{8\gamma}\right) F_{av}(\sigma) \Delta q^* \quad (2)$$

where:

$$G_{av}(\sigma) = \frac{2G_s(\sigma)}{J_o(\sqrt{-\sigma})} \int_0^1 y J_o(y\sqrt{-\sigma}) dy = \frac{2G_s(\sigma)}{J_o(\sqrt{-\sigma})} \frac{J_1(\sqrt{-\sigma})}{\sqrt{-\sigma}} = \frac{G_s(\sigma)}{\sigma Z(\sigma)} = F_s(\sigma) \quad (3)$$

$$F_{av}(\sigma) = \frac{1}{1 + \frac{1}{8\gamma}} \quad \frac{1}{\gamma \sigma} \quad [1 - G_{av}(\sigma)] \quad (4)$$

Appendix 3 - Solution of the characteristic equation

The characteristic equation is the following:

$$1 + \frac{\gamma}{Z(\sigma)} = 0 \quad (1)$$

with:

$$Z(\sigma) = - \frac{J_o(\sqrt{-\sigma})}{2\sqrt{-\sigma} J_1(\sqrt{-\sigma})} = \frac{d \lg [\sqrt{-\sigma} J_1(\sqrt{-\sigma})]}{d\sigma} \quad (2)$$

Equation (1) can be written as follows:

$$\frac{d \lg [\sqrt{-\sigma} J_1(\sqrt{-\sigma})]}{d\sigma} = -\gamma \quad (3)$$

It is:

$$J_1(\sqrt{-\sigma}) = \frac{\sqrt{-\sigma}}{2} \prod_{n=2}^{\infty} \left(1 + \frac{\sigma}{b_n}\right) \quad (4)$$

where $\sqrt{b_n}$ are the real zeros of the Bessel function J_1 .

Equation (3) can be written:

$$\frac{1}{\sigma} + \sum_{n=2}^{\infty} \frac{\frac{1}{b_n}}{1 + \frac{\sigma}{b_n}} = -\gamma \quad (5)$$

with all the b_n real and positive.

If $\sigma = x + iy$ is a root of equation (5), then, putting it in (5), the imaginary part must be equal to zero, that is:

$$y \left[\frac{1}{x^2 + y^2} + \sum_{n=2}^{\infty} \frac{1/b_n^2}{(1+x/b_n)^2 + y^2/b_n^2} \right] = 0 \quad (6)$$

Equation (6) is satisfied only if:

$$y = 0 \quad (7)$$

From (7) we can conclude that all the roots of the characteristic equation (1) are real. Since the coefficients of equation (1) are all positive, the roots will also be all negative.

Fig.27 shows the function $Z(\sigma)$ plotted against negative values of σ on logarithmic scales. The roots are given by the intersection of the curve $Z(\sigma)$ with the horizontal lines $\gamma = \text{constant}$.

Eq.(1) has been programmed on a digital computer IBM 7070 and its roots, $-\sigma_n$, have been calculated up to the value $n=20$ for values of γ between 10^{-4} and 10.

Fig.2 shows the normalized values, $\bar{\sigma}_n$, as function of γ . The relationship between σ_n and $\bar{\sigma}_n$ is the following:

$$\sigma_n = b_n + (a_n - b_n) \bar{\sigma}_n \quad (8)$$

where $\sqrt{a_n}$ and $\sqrt{b_n}$ are respectively the n-th zeros of the Bessel functions J_0 and J_1 . The values of the coefficients a_n and b_n are given in table 1.

It is interesting to know that

$$\lim_{\gamma \rightarrow \infty} \sigma_1 = \frac{1}{\gamma} \quad (9)$$

and therefore

$$\lim_{\gamma \rightarrow \infty} \tilde{\sigma}_1 = \frac{1}{a_1 \gamma} \quad (10)$$

being $b_1 = 0$ (table 1)

Appendix 4 - Evaluation of the coefficients associated to the series of exponentials

We shall start with the coefficients δ_{sn} from eq.(29) par.3. δ_{sn} is calculated in the following way:

$$\begin{aligned} \delta_{sn} &= \lim_{\sigma \rightarrow -\sigma_n} G_s(\sigma) \left(1 + \frac{\sigma}{\sigma_n}\right) = \lim_{\sigma \rightarrow -\sigma_n} \frac{1 + \frac{\sigma}{\sigma_n}}{1 + \frac{\gamma}{Z(\sigma)}} = \\ &= \lim_{\sigma \rightarrow -\sigma_n} \frac{\left(1 + \frac{\sigma}{\sigma_n}\right) J_0(\sqrt{-\sigma})}{J_0(\sqrt{-\sigma}) - 2\gamma \sqrt{-\sigma} J_1(\sqrt{-\sigma})} = J_0(\sqrt{\sigma_n}) \frac{\frac{1}{\sigma_n}}{\frac{J_1(\sqrt{\sigma_n})}{2\sqrt{\sigma_n}} + \gamma J_0(\sqrt{\sigma_n})} = \\ &= \frac{1}{\sigma_n} \frac{1}{\gamma - \frac{1}{4 \sigma_n Z(-\sigma_n)}} \end{aligned} \quad (1)$$

With reference to eq.(1) in Appendix 3

$$Z(\sqrt{-\sigma_n}) = -\gamma \quad (2)$$

the final expression is:

$$\delta_{sn} = \frac{\gamma}{0.25 + \gamma^2 \sigma_n} \quad (3)$$

We obtain:

a) from eqs.(24) and (39)

$$\epsilon_{sn} = \frac{\delta_{sn}}{\gamma \sigma_n} = \frac{1}{\sigma_n (0.25 + \gamma^2 \sigma_n)} \quad (4)$$

b) from eqs.(25) and (31)

$$\delta_{cn} = \frac{\delta_{sn}}{J_o(\sqrt{\sigma_n})} = \frac{\gamma}{0.25 + \gamma^2 \sigma_n} \cdot \frac{1}{J_o(\sqrt{\sigma_n})} \quad (5)$$

c) from eqs.(26) and (32)

$$\epsilon_{cn} = \frac{1}{1 + \frac{1}{4\gamma}} \cdot \frac{\delta_{cn}}{\gamma \sigma_n} = \frac{4\gamma}{1+4\gamma} \cdot \frac{1}{\sigma_n (0.25 + \gamma^2 \sigma_n)} - \frac{1}{J_o(\sqrt{\sigma_n})} \quad (6)$$

d) from eqs.(28) and (36)

$$\mu_n = \frac{1}{1 + \frac{1}{8\gamma}} \cdot \frac{\epsilon_{sn}}{\gamma \sigma_n} = \frac{8}{1+8\gamma} \cdot \frac{1}{\sigma_n^2 (0.25 + \gamma^2 \sigma_n)} \quad (7)$$

e) from eqs.(17), (25) and (33)

$$\delta_n = \delta_{cn} J_o(y\sqrt{\sigma_n}) = \frac{\gamma}{0.25 + \gamma^2 \sigma_n} \cdot \frac{J_o(y\sqrt{\sigma_n})}{J_o(\sqrt{\sigma_n})} \quad (8)$$

f) from eqs.(19), (33) and (34)

$$\epsilon_n = \frac{1 + \frac{1}{4\gamma}}{1 + \frac{1-y^2}{4\gamma}} \cdot \epsilon_{cn} J_o(y\sqrt{\sigma_n}) = \frac{4\gamma}{1-y^2+4\gamma} \cdot \frac{1}{\sigma_n (0.25 + \gamma^2 \sigma_n)} \cdot \frac{J_o(y\sqrt{\sigma_n})}{J_o(\sqrt{\sigma_n})} \quad (9)$$

Appendix 5 - Antitransformation by using for $Z(\sigma)$ the approximate expression $R(\sigma)$

From (73) of par. 6, it is:

$$\frac{1}{\sigma} G_s(\sigma) \approx \frac{1}{\sigma} \frac{\sqrt{1+0.25\sigma}}{\sqrt{1+0.25\sigma} + \gamma\sigma} \quad (1)$$

(1) can be written as follows:

$$\begin{aligned} \frac{1}{\sigma} G_s(\sigma) = & \frac{1}{\sigma} - \frac{c_1}{c_1 - c_2} \frac{1}{\sigma + c_1} - \frac{1}{2\gamma(c_1 - c_2)} \frac{\sqrt{\sigma + 4}}{\sigma + c_1} - \frac{c_2}{c_2 - c_1} \frac{1}{\sigma + c_2} - \\ & - \frac{1}{2\gamma(c_2 - c_1)} \frac{\sqrt{\sigma + 4}}{\sigma + c_2} \end{aligned} \quad (2)$$

where:

$$c_1 = \frac{1}{\gamma} (\beta - \alpha) \quad (3)$$

$$c_2 = -\frac{1}{\gamma} (\beta + \alpha) \quad (4)$$

$$\alpha = \frac{0.125}{\gamma} \quad (5)$$

$$\beta = \sqrt{1+\alpha^2} \quad (6)$$

Taking into account that:

$$L^{-1}\left(\frac{1}{\sigma}\right) = 1(\tau) \quad (7)$$

$$L^{-1}\left(\frac{c_1}{c_1 - c_2} \frac{1}{\sigma + c_1}\right) = \frac{c_1}{c_1 - c_2} e^{-c_1 \tau} = \frac{\beta - \alpha}{2\beta} e^{-\frac{\beta - \alpha}{\gamma} \tau} \quad (8)$$

$$\begin{aligned} L^{-1} \left[\frac{1}{2\gamma(c_1 - c_2)} \frac{\sqrt{\sigma+4}}{\sigma+c_1} \right] &= \frac{1}{2\gamma(c_1 - c_2)} \left[\sqrt{\pi\tau} e^{-4\tau} + \sqrt{(4-c_1)} e^{-c_1\tau} E(\sqrt{4-c_1}\sqrt{\tau}) \right] = \\ &= \frac{\sqrt{\pi\tau}}{4\beta} e^{-4\tau} + \frac{\beta-\alpha}{2\beta} e^{-\frac{\beta-\alpha}{\gamma}\tau} E[2(\beta-\alpha)\sqrt{\tau}] \end{aligned} \quad (9)$$

$$L^{-1} \left[\frac{c_2}{c_2 - c_1} \frac{1}{\sigma + c_2} \right] = \frac{c_2}{c_2 - c_1} e^{-c_2\tau} = \frac{\beta+\alpha}{2\beta} e^{-\frac{\beta+\alpha}{\gamma}\tau} \quad (10)$$

$$\begin{aligned} L^{-1} \left[\frac{1}{2\gamma(c_2 - c_1)} \frac{\sqrt{\sigma+4}}{\sigma+c_2} \right] &= \frac{1}{2\gamma(c_2 - c_1)} \left[\sqrt{\pi\tau} + \sqrt{(4-c_2)} e^{-c_2\tau} E(\sqrt{4-c_2}\sqrt{\tau}) \right] = \\ &= -\frac{\sqrt{\pi\tau}}{4\beta} - \frac{\beta+\alpha}{2\beta} e^{-\frac{\beta+\alpha}{\gamma}\tau} E[2(\beta+\alpha)\sqrt{\tau}] \end{aligned} \quad (11)$$

We obtain:

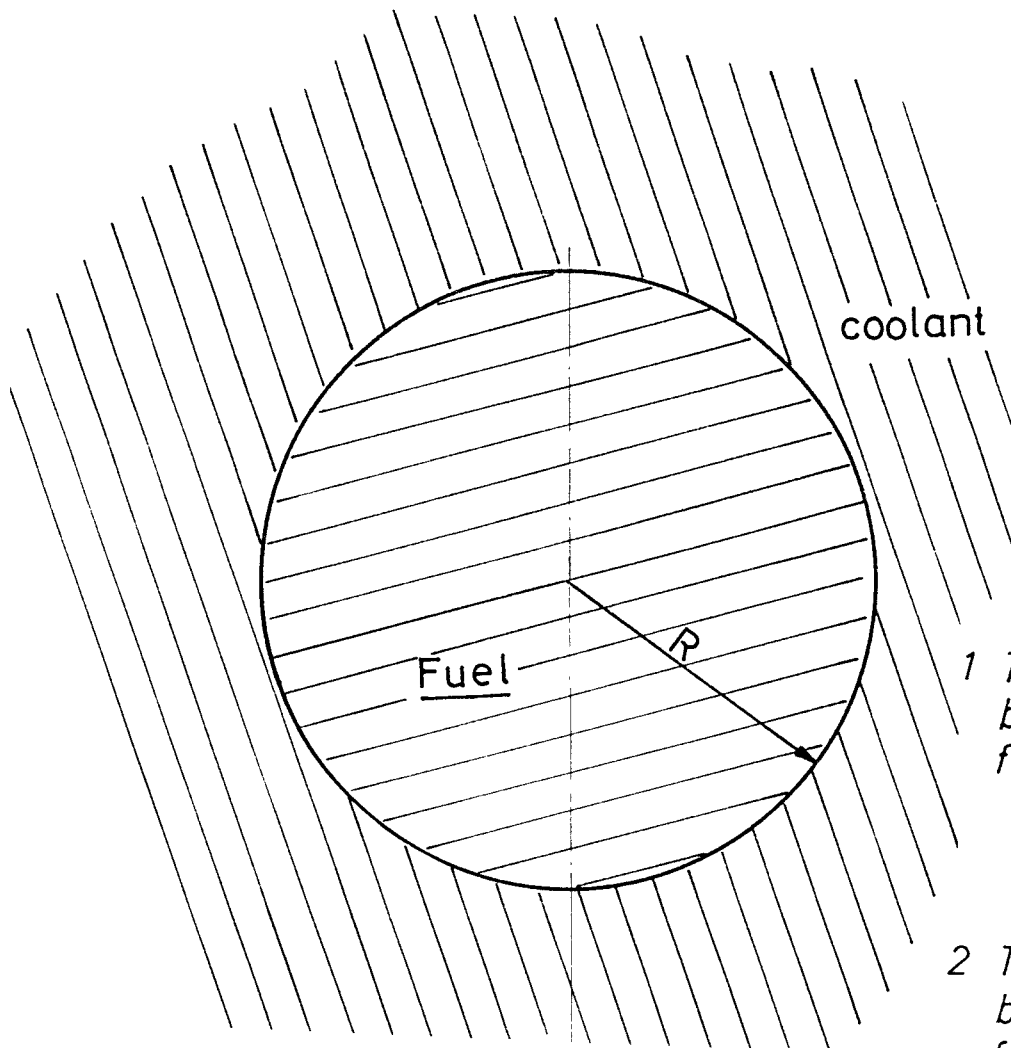
$$\begin{aligned} L^{-1} \left[\frac{1}{\sigma} G_s(\sigma) \right] &= 1(\tau) - \frac{\beta-\alpha}{2\beta} e^{-\frac{\beta-\alpha}{\gamma}\tau} \left[1 + E[2(\beta-\alpha)\sqrt{\tau}] \right] - \\ &- \frac{\beta+\alpha}{2\beta} e^{-\frac{\beta+\alpha}{\gamma}\tau} \left[1 - E[2(\beta+\alpha)\sqrt{\tau}] \right] \end{aligned} \quad (12)$$

(9) and (10) have been calculated according to Bibl.5, vol.1, p.235, Nr.22.

The antittransformed of $\frac{1}{\sigma} F_s(\sigma)$ and $\frac{1}{\sigma} F_{av}(\sigma)$ can be calculated in the same way or by integration of $L^{-1}(\frac{1}{\sigma} G_s(\sigma))$ in the time domain using respectively eqs.(24) and (28) of par.2.

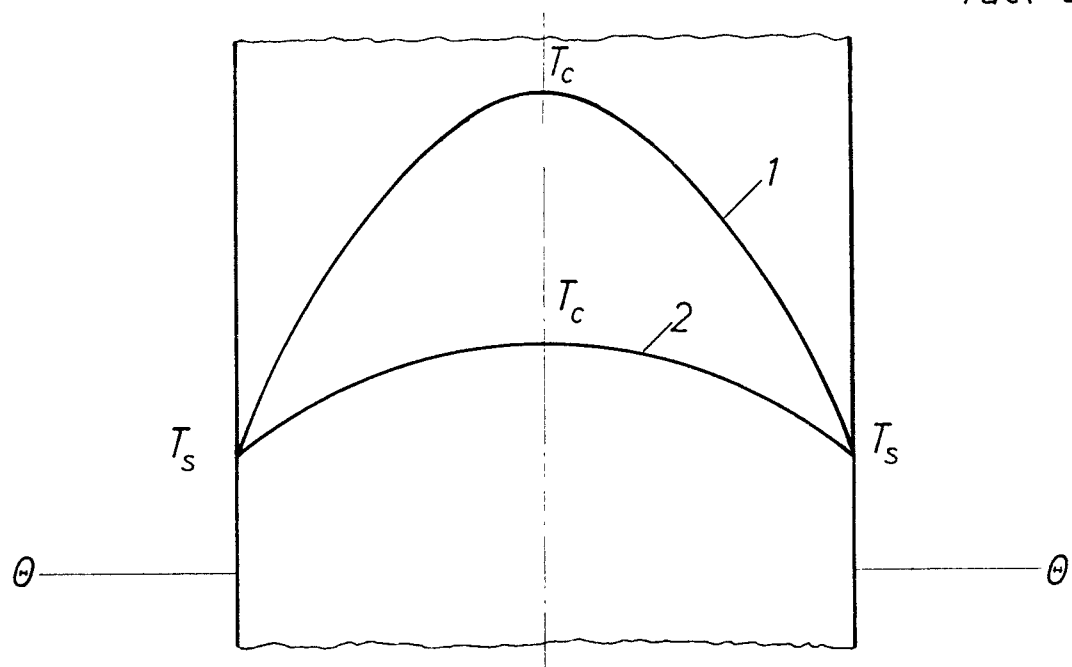
Bibliography

- 1) N.W.McLachlan "Bessel Functions for Engineers"
The Oxford Engineering Science Series
- 2) Jahnke - Emde "Tables of Higher Functions"
- 3) L.Caldarola and C.Zaffiro "Transitori Termici in Simmetria
Cilindrica" Rendiconti A.E.I.1959
- 4) F.Storrer "Temperature Response to Power, Inlet Coolant Temperature
and Flow Transients in Solid Fuel Reactors" APDA 132
- 5) Bateman Manuscript Project: "Tables of Integral Transforms"
McGraw Hill Book Co.
- 6) Häfele, Ott, Caldarola, Schikarski and Cohen, Wolfe, Greebler
and Reynolds: "Static and Dynamic Measurements on the Doppler
Effect in an Experimental Fast Reactor" Geneva Conference 1964
- 7) Cohen, Greebler, Horst and Wolfe: "The Southwest Experimental
Fast Oxyde Reactor" APED-4281 Class 1, August 1963



1 Temperature Distribution in a ceramic fuel element

2 Temperature Distribution in a metallic fuel element



System Geometry

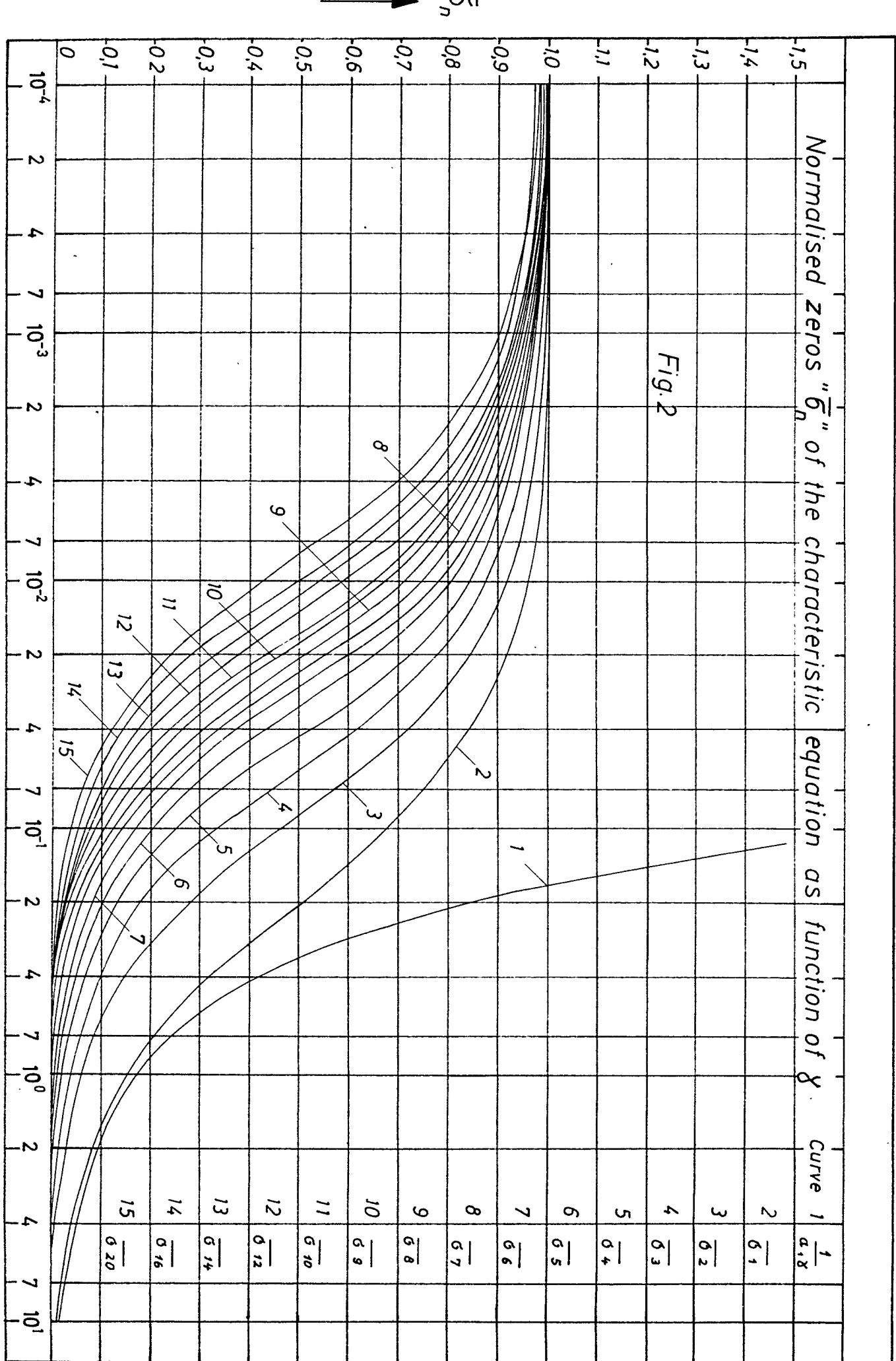
Fig. 1

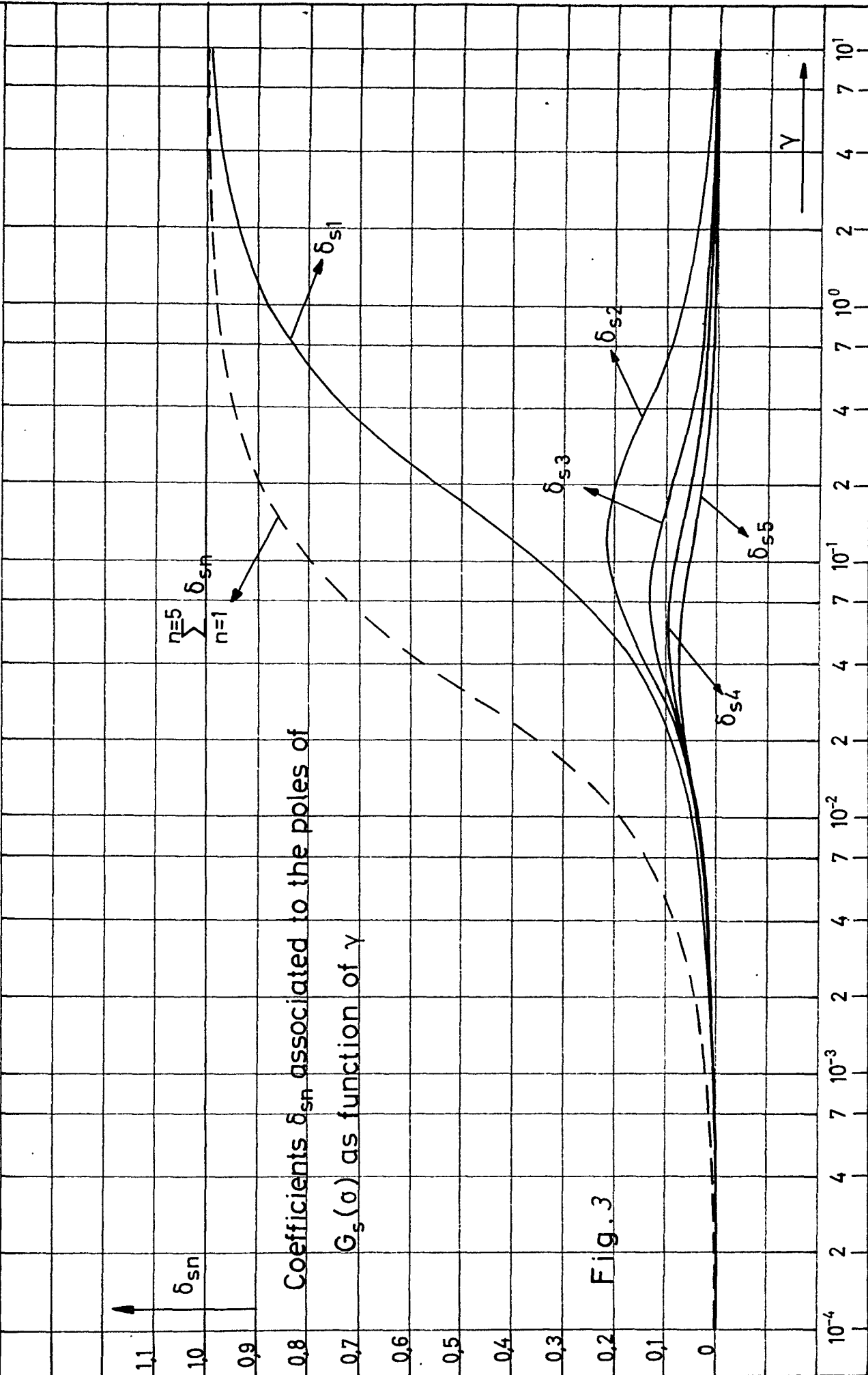
Normalised zeros " $\bar{\sigma}_n$ " of the characteristic equation as function of γ .

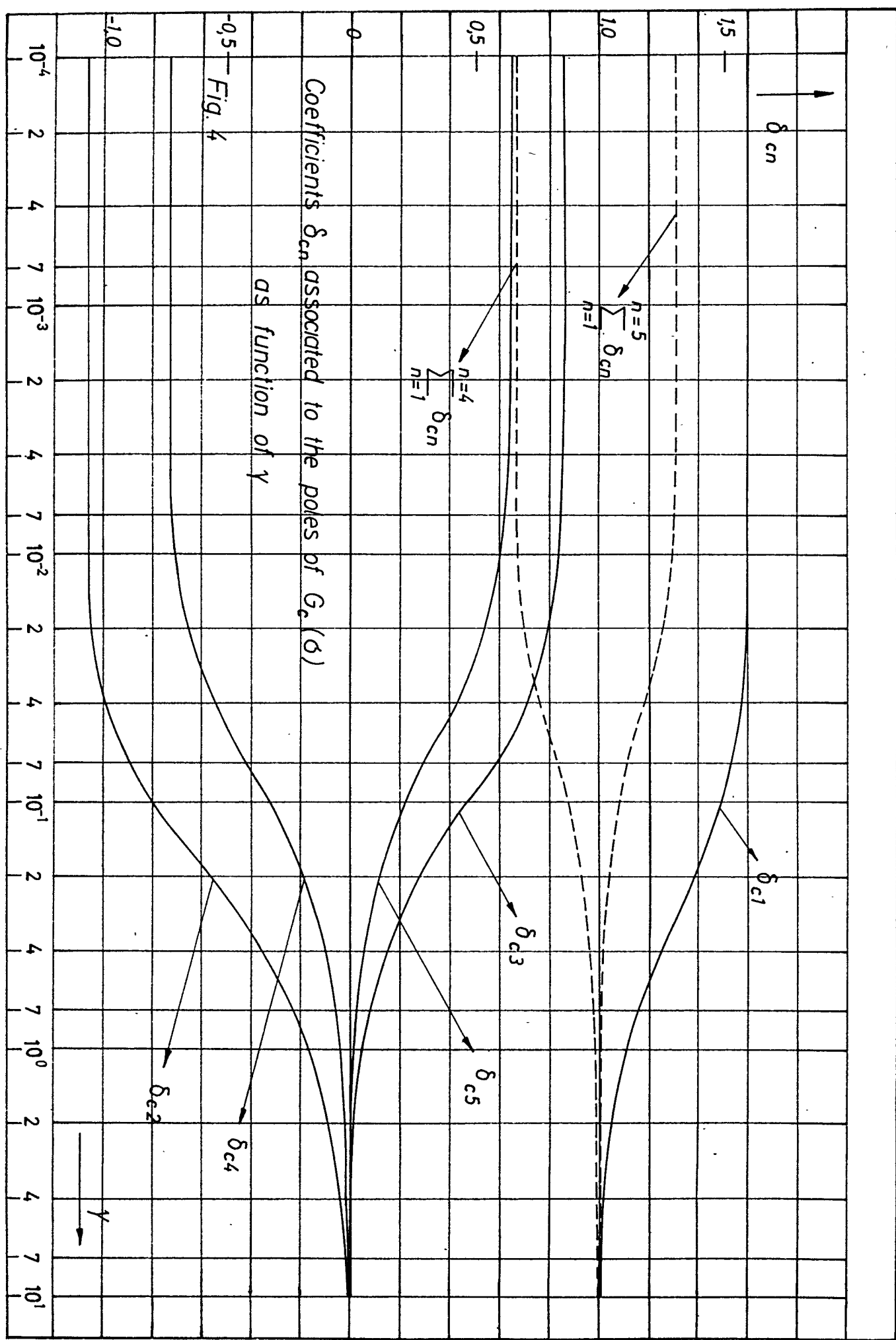
$$\text{Curve } 1 \frac{1}{\alpha_1 \gamma}$$

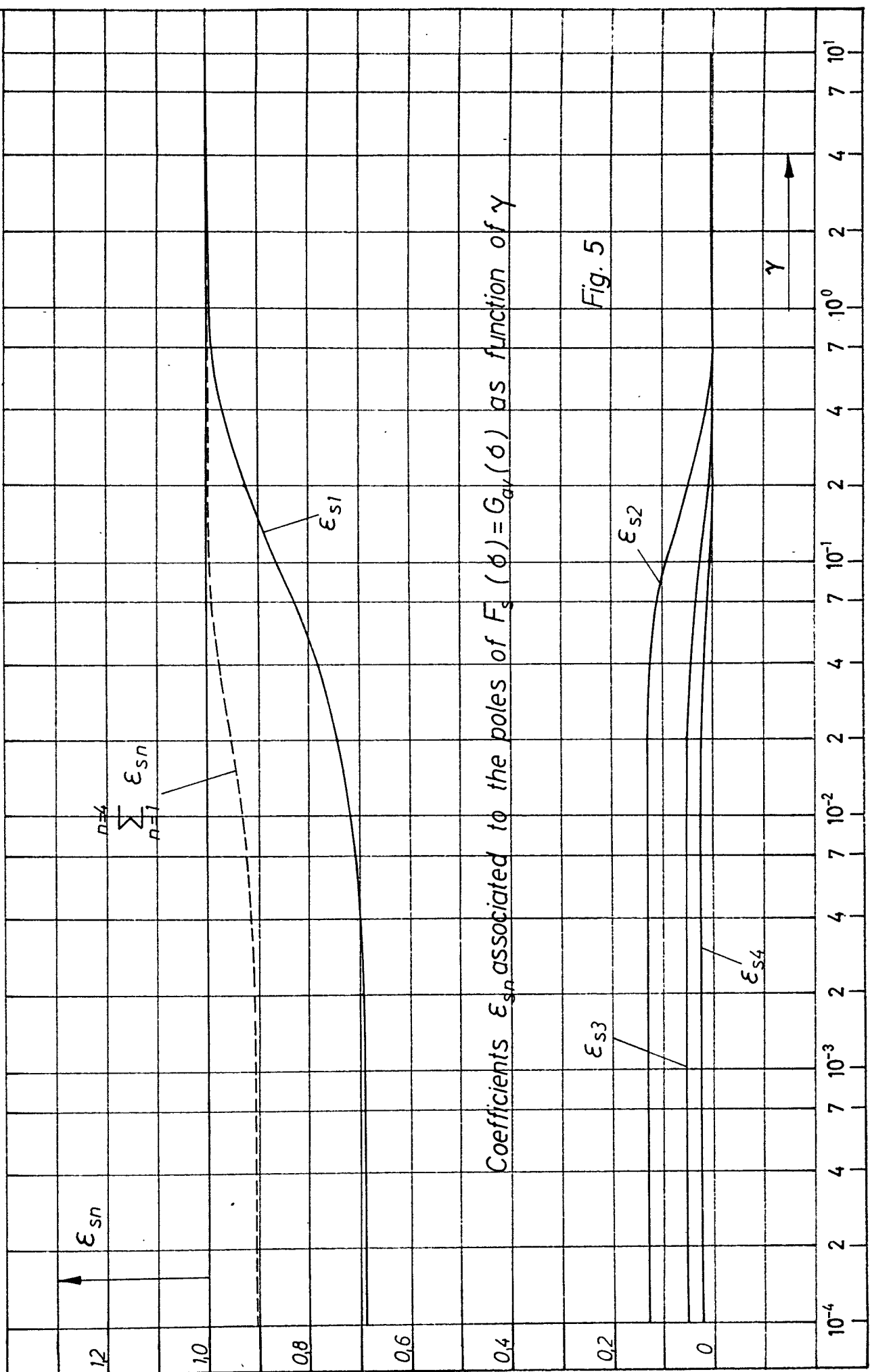
1.5	2	$\frac{1}{\alpha_1}$
1.4	3	$\frac{1}{\alpha_2}$
1.3	4	$\frac{1}{\alpha_3}$
1.2	5	$\frac{1}{\alpha_4}$
1.1	6	$\frac{1}{\alpha_5}$
1.0	7	$\frac{1}{\alpha_6}$
0.9	8	$\frac{1}{\alpha_7}$
0.8	9	$\frac{1}{\alpha_8}$
0.7	10	$\frac{1}{\alpha_9}$
0.6	11	$\frac{1}{\alpha_{10}}$
0.5	12	$\frac{1}{\alpha_{11}}$
0.4	13	$\frac{1}{\alpha_{12}}$
0.3	14	$\frac{1}{\alpha_{13}}$
0.2	15	$\frac{1}{\alpha_{14}}$
0.1	16	$\frac{1}{\alpha_{15}}$
0	17	$\frac{1}{\alpha_{16}}$

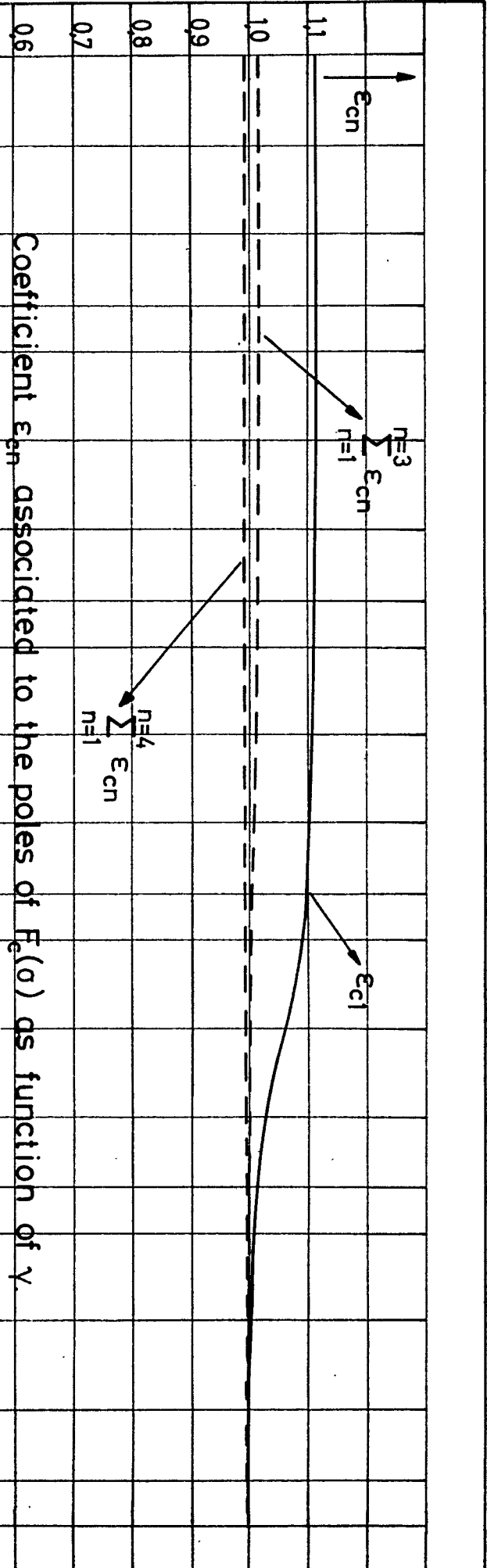
Fig. 2





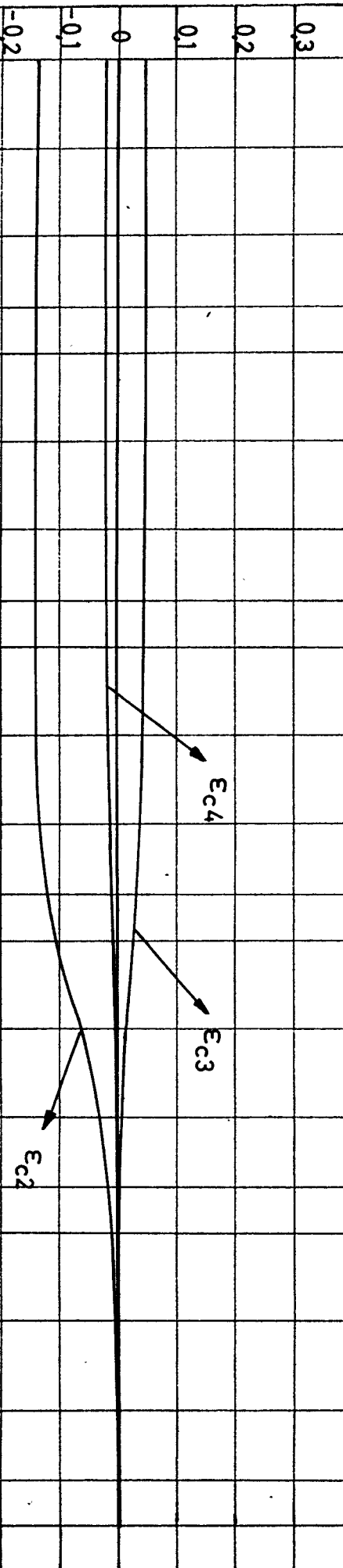


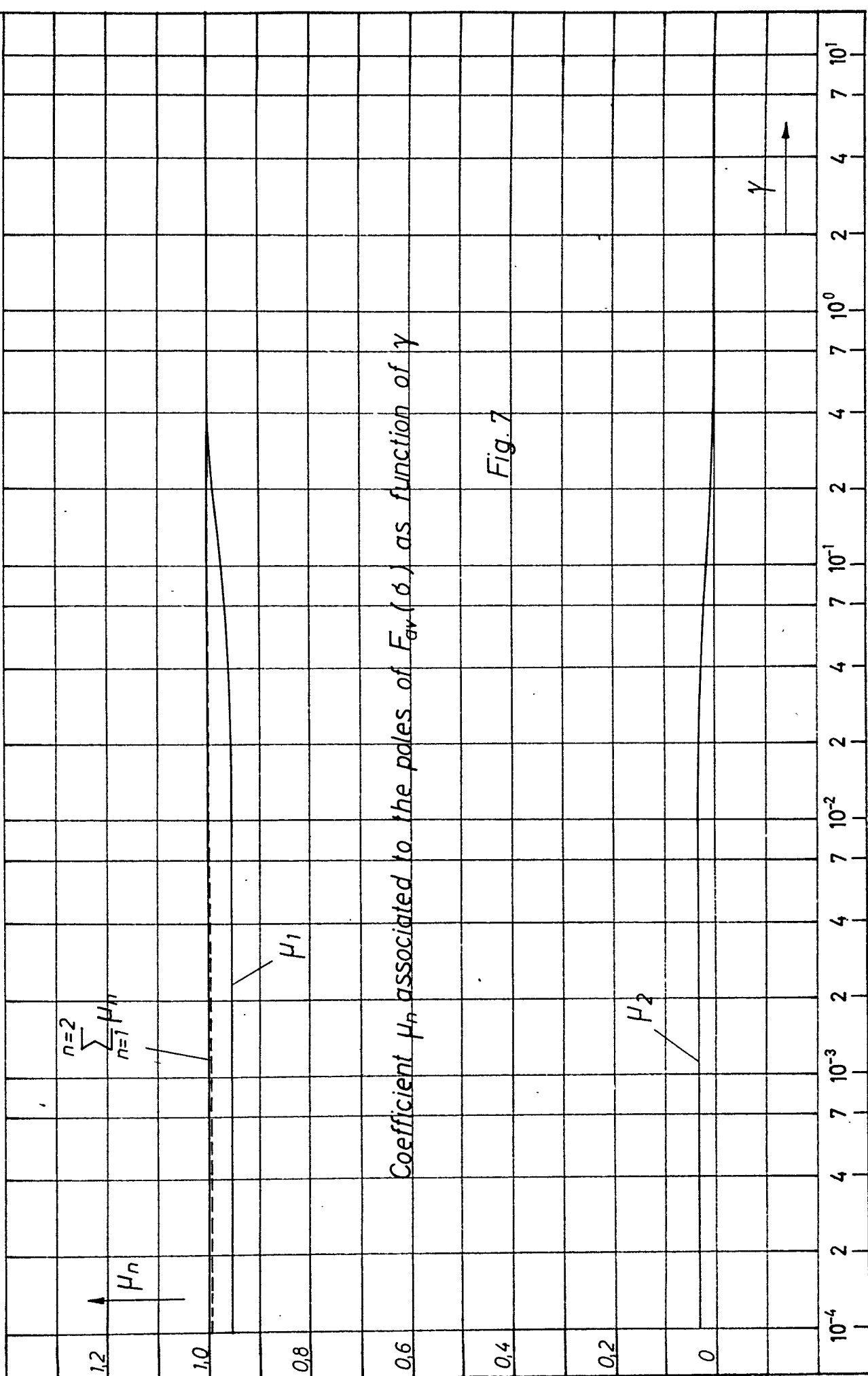




Coefficient ϵ_{cn} associated to the poles of $F_e(\sigma)$ as function of γ .

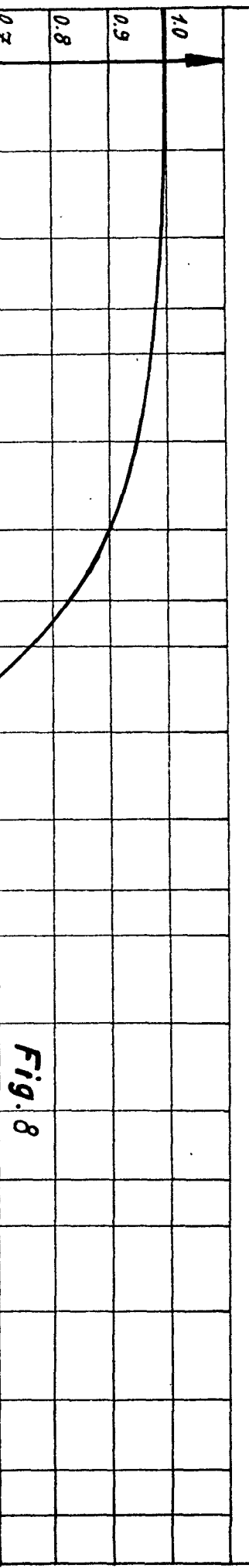
Fig. 6





Coefficient μ_n associated to the poles of $F_{\text{av}}(\delta)$ as function of γ

Fig. 7



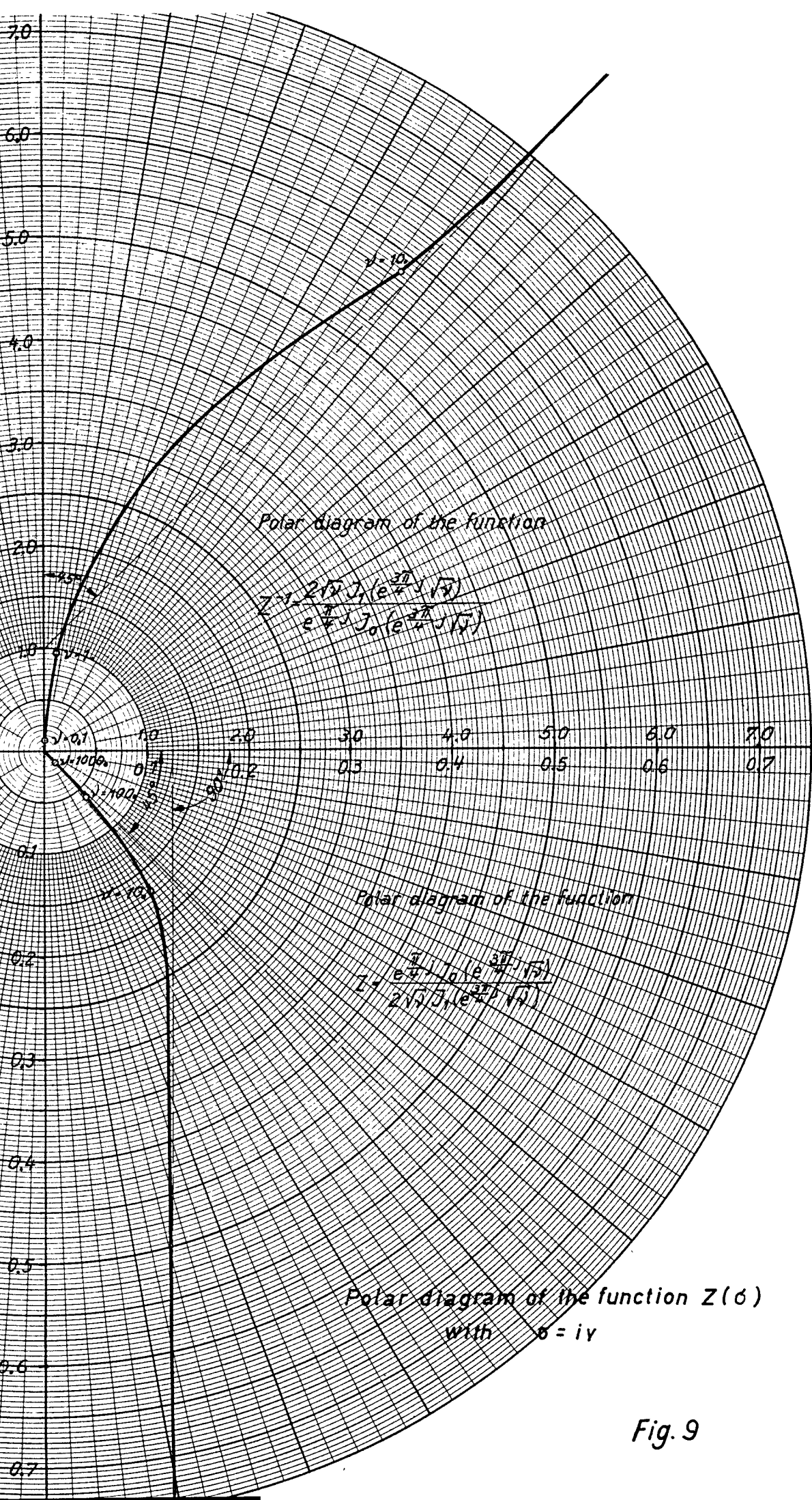
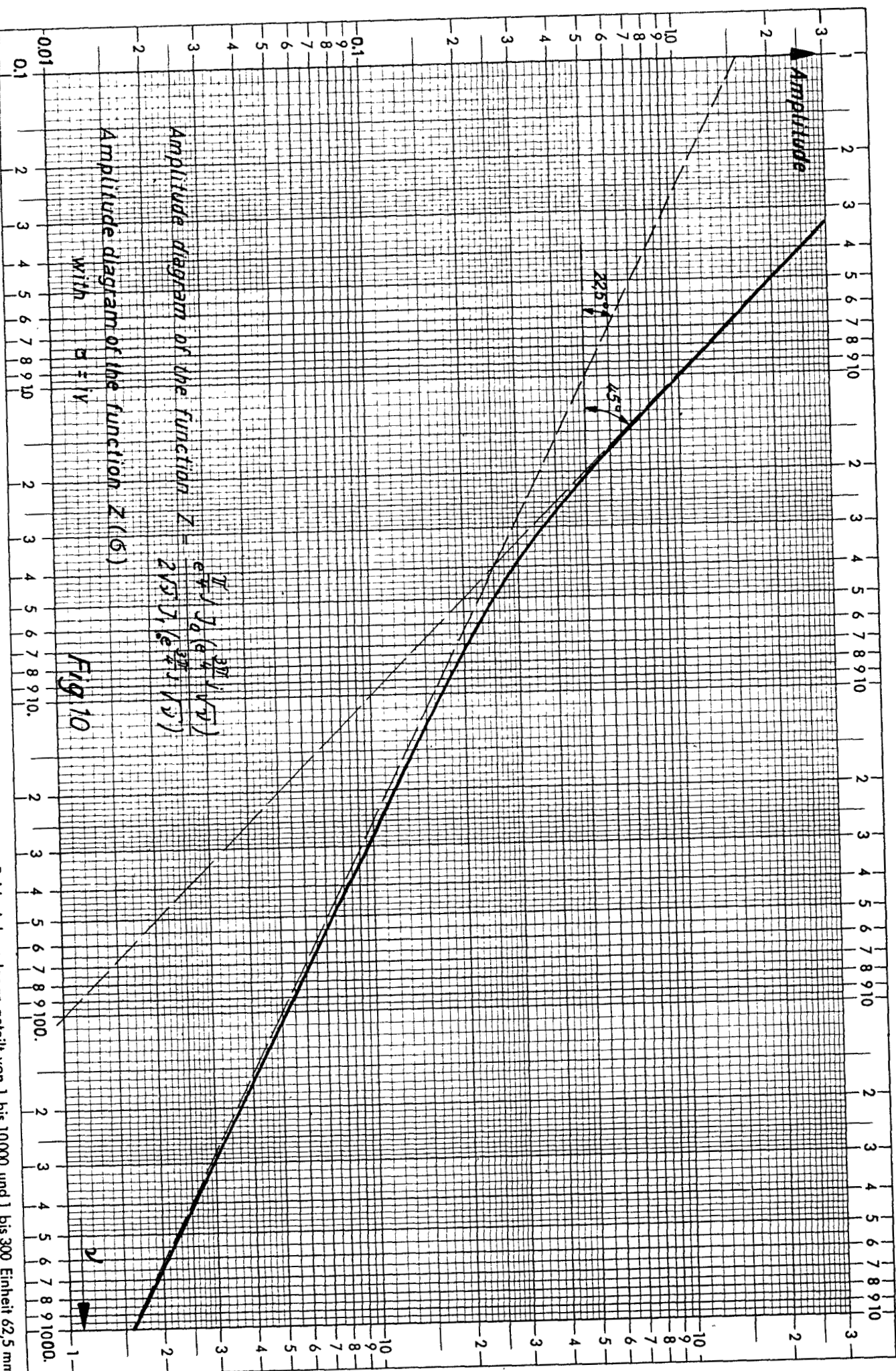
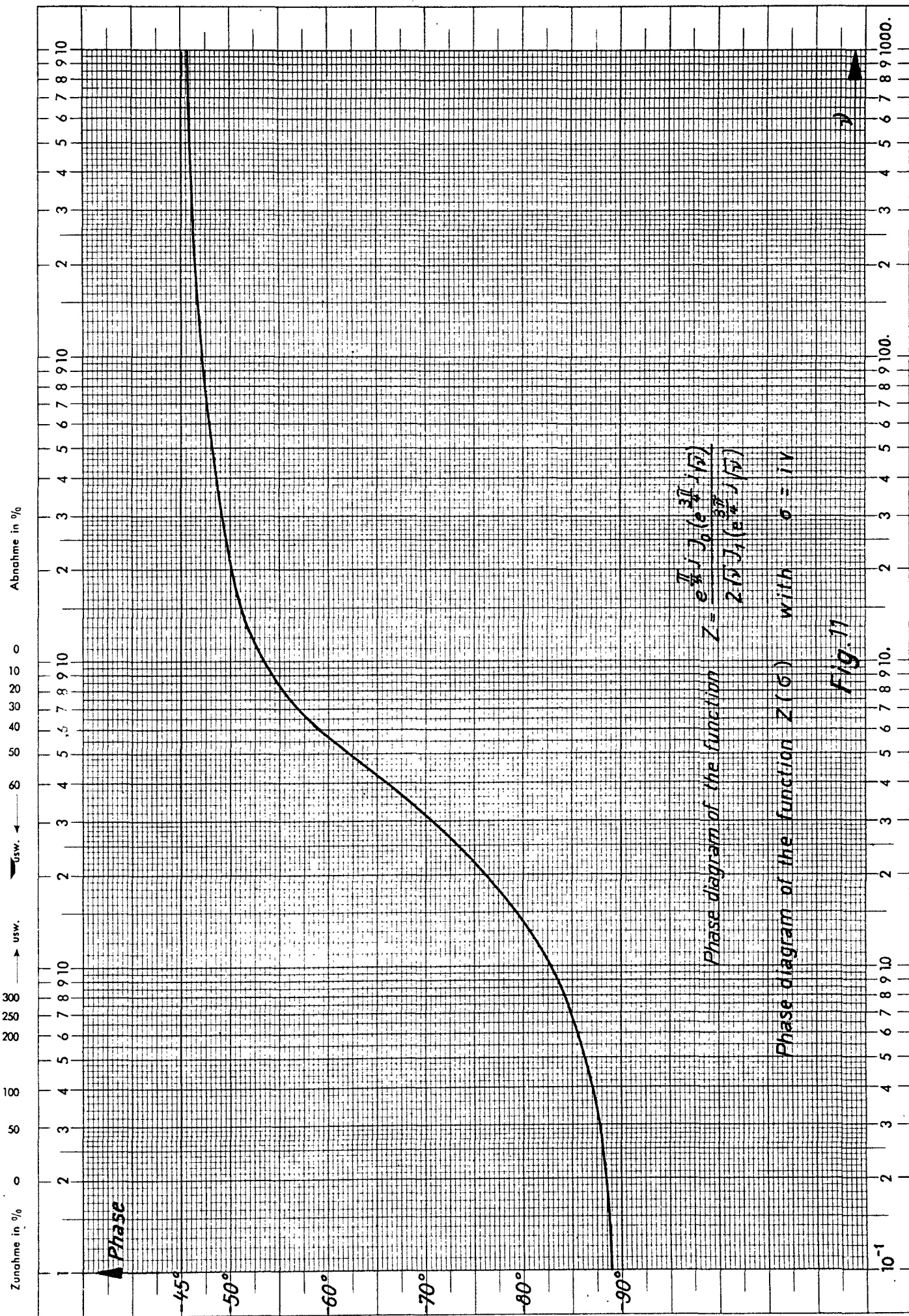


Fig. 9



Beide Achsen logar. geteilt von 1 bis 10000 und 1 bis 300 Einheit 62,5 mm



Approximation of $Z(v)$ with $R(v)$

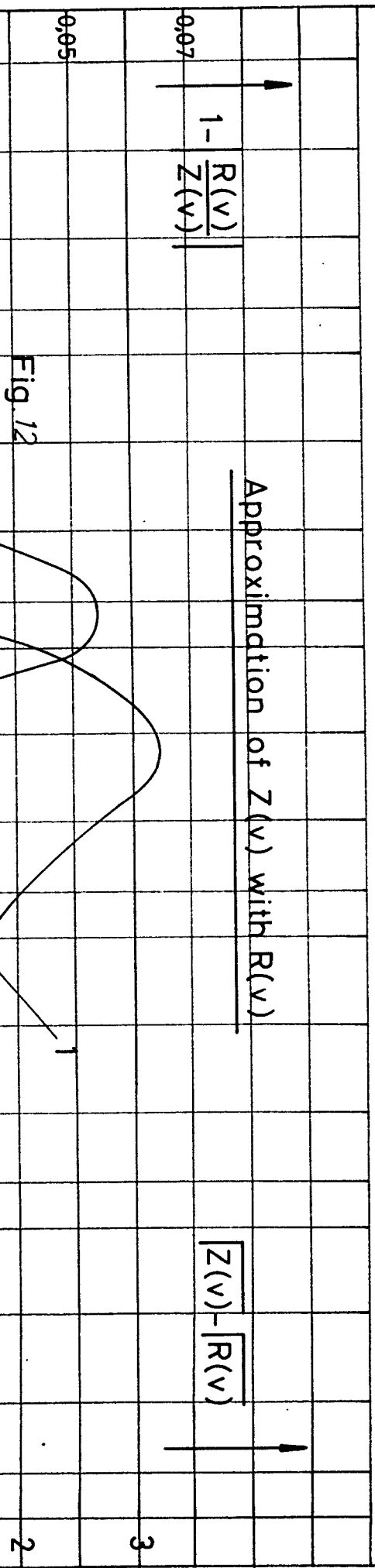
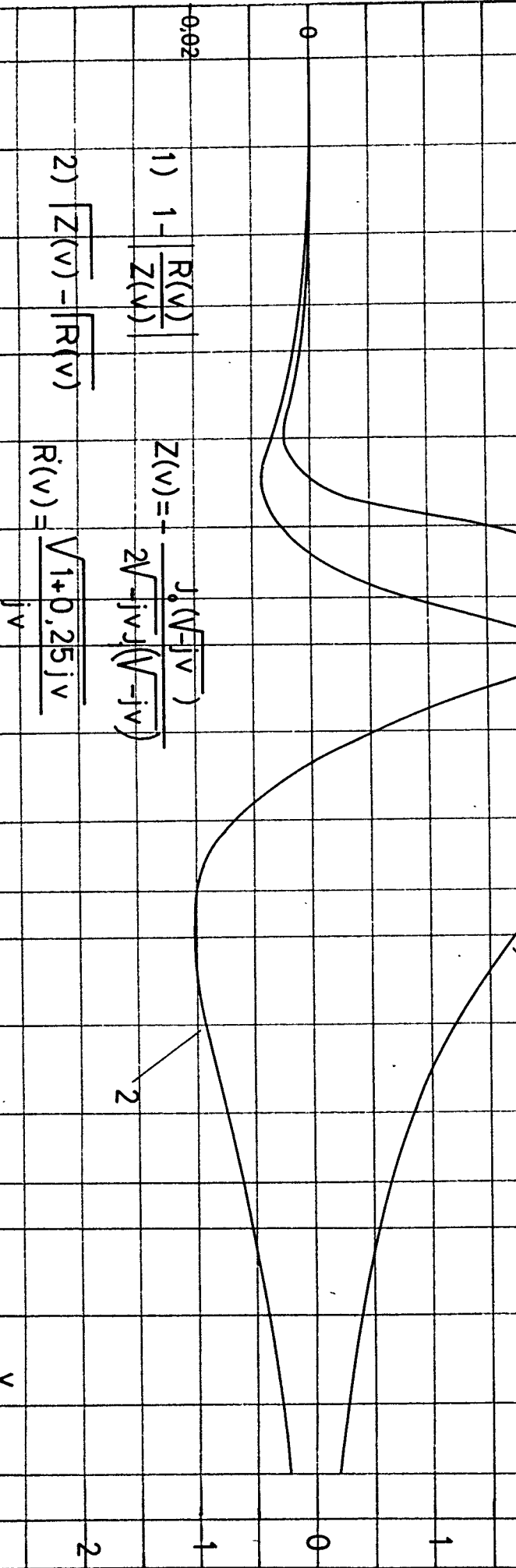


Fig. 12



$$1) \quad 1 - \frac{R(v)}{Z(v)} = \frac{J_0(\sqrt{-jv})}{2\sqrt{-jv}J(\sqrt{-jv})}$$

$$2) \quad [Z(v) - R(v)] = \frac{\sqrt{1+0.25jv}}{jv}$$

$10^1 \quad 2 \quad 4 \quad 7 \quad 10^0 \quad 2 \quad 4 \quad 7 \quad 10^1 \quad 2 \quad 4 \quad 7 \quad 10^2 \quad 2 \quad 4 \quad 7 \quad 10^3 \quad 2 \quad 4 \quad 7 \quad 10^4$

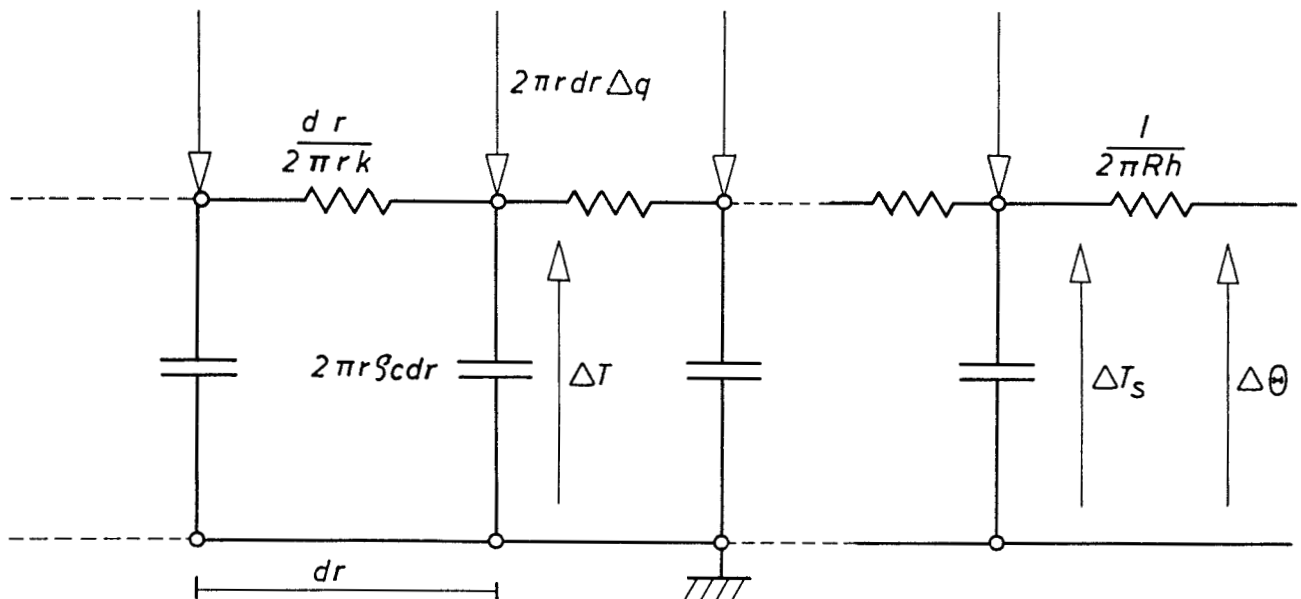


Fig. 13 A

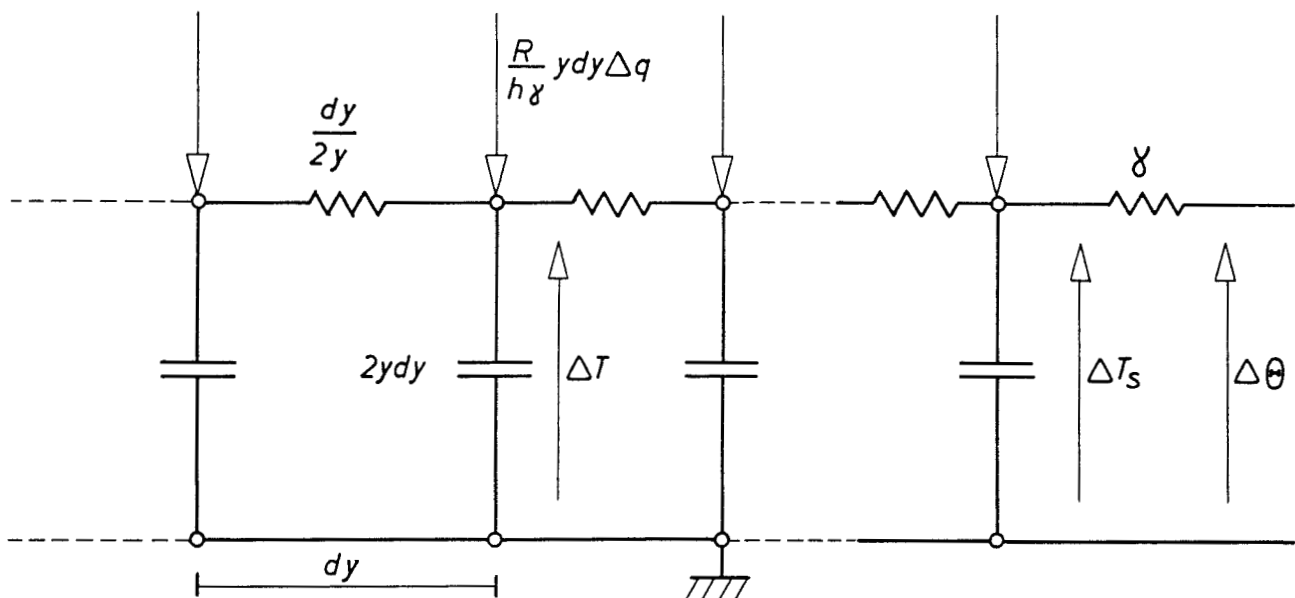


Fig. 13 B

Fig. 13

Electrical Analogy

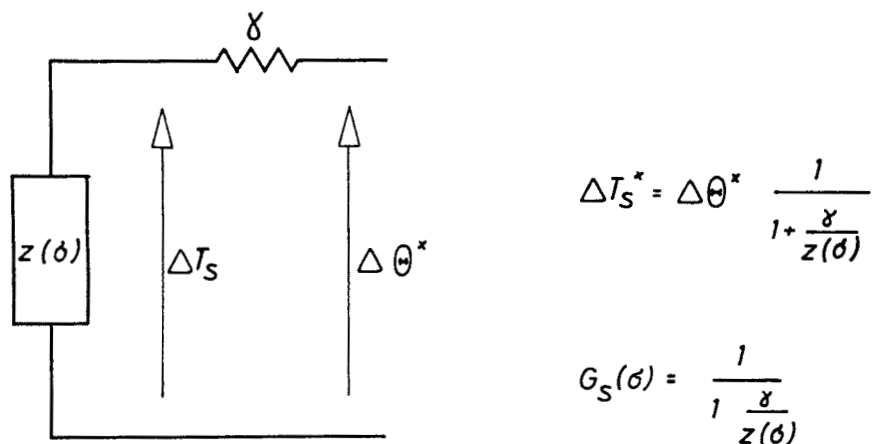


Fig. 14 A

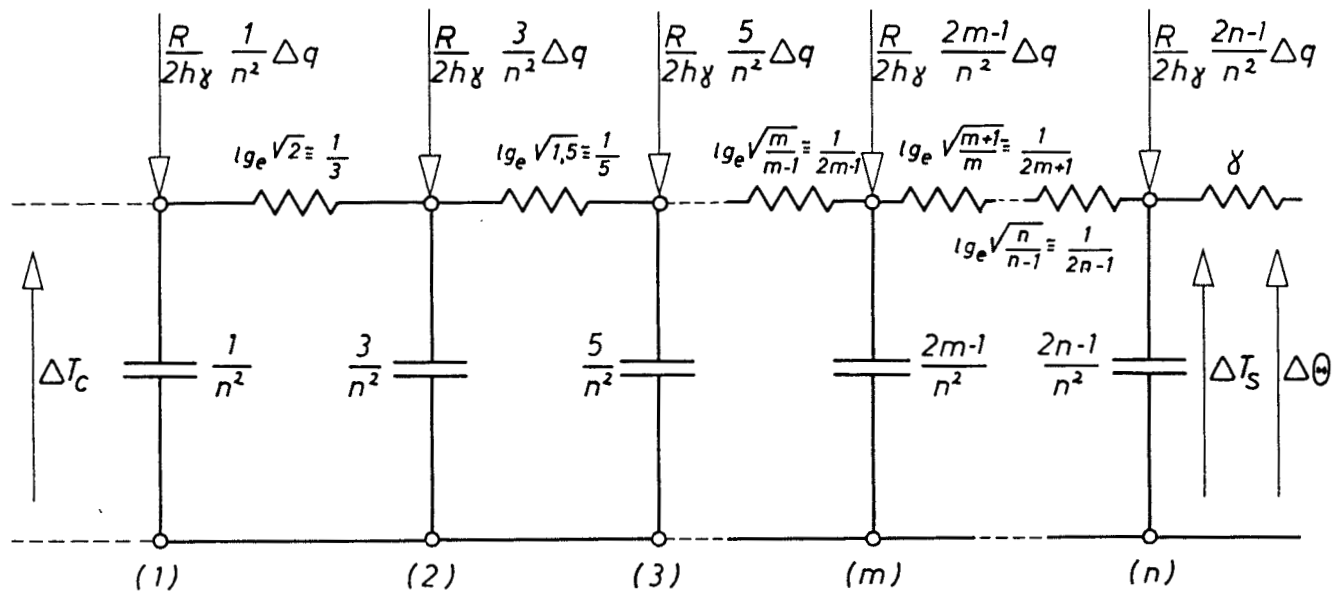
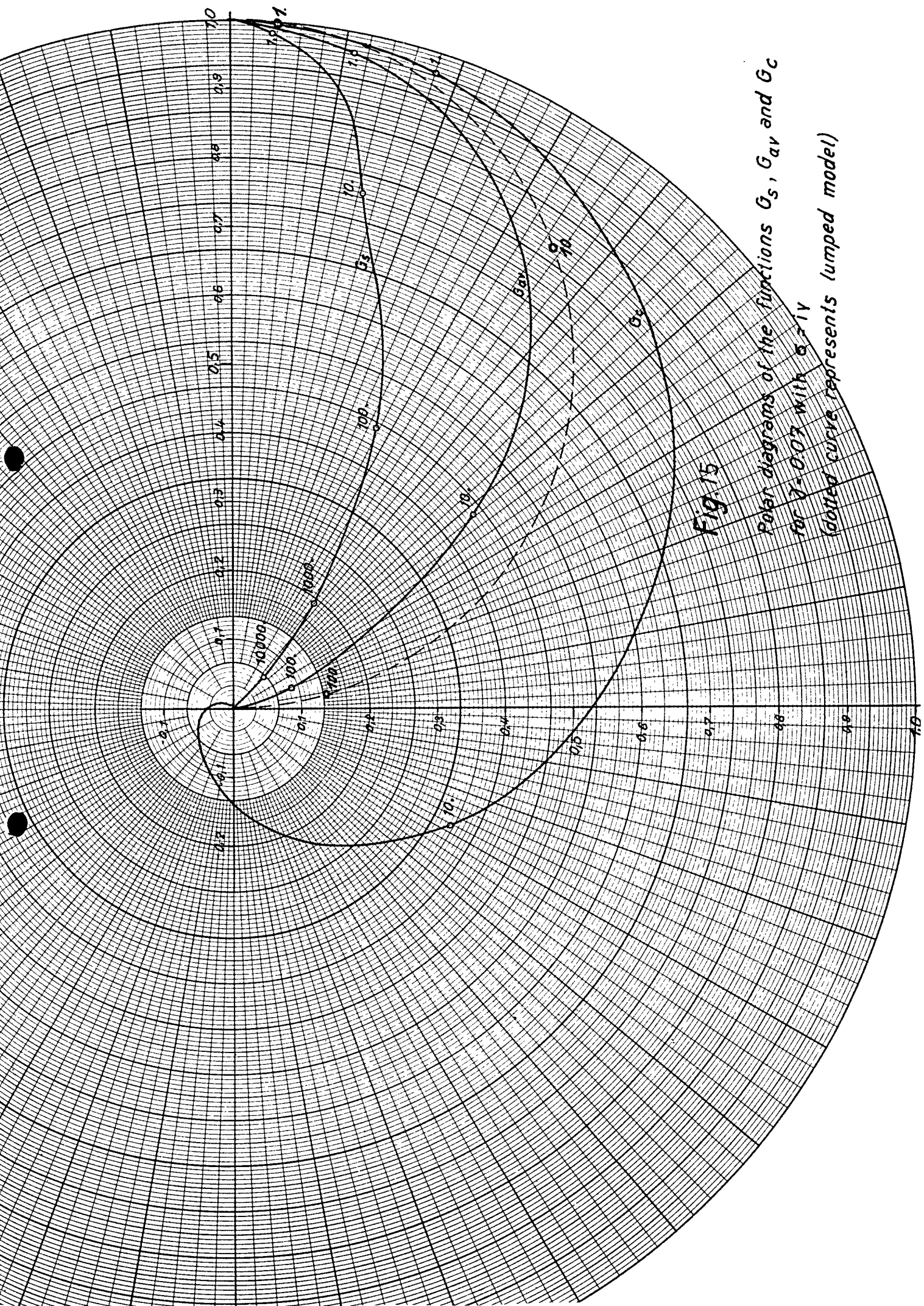


Fig. 14 B

Fig. 14

Electrical Analogy

Fig 15
 polar diagrams of the functions G_s , G_{av} and G_c
 for $\delta = 0.07$ with $\zeta = 1/V$
 (dotted curve represents lumped model)



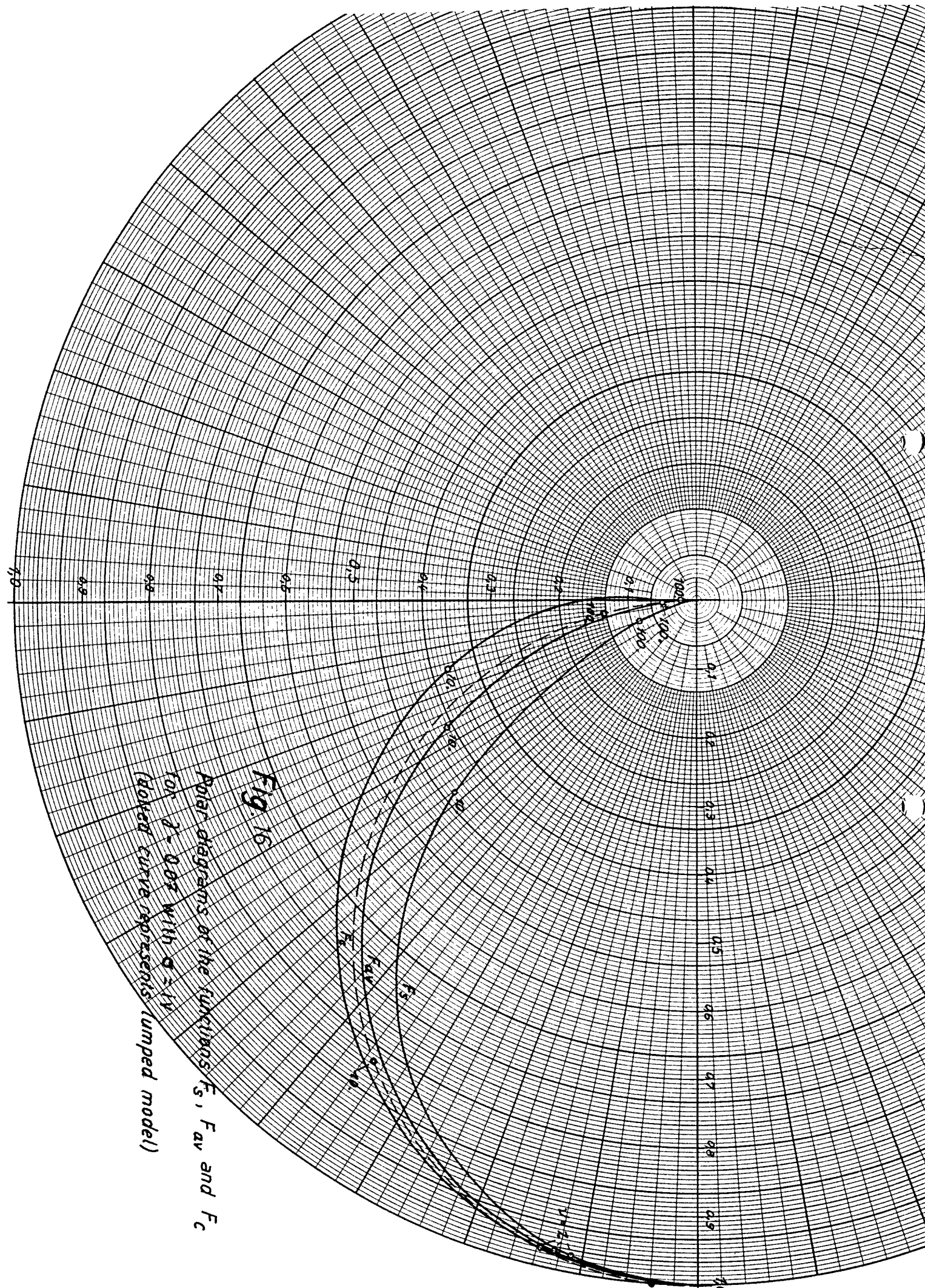


Fig. 16
Dependence of the functions F_s , F_{av} and F_c
on r_{10} with $\sigma = 1/4$
(broken curve represents lumped model)

$$\frac{\Delta T_{av}}{\Delta P} \left[^\circ C / MW \right]$$

$$-1 \left[\frac{1}{\sigma} F_{av}(\sigma) \right]$$

$$4.35 - 1.0$$

Approximated curves of the antitransformed

of the function $\frac{1}{\sigma} F_{av}(\sigma)$ in the case $\gamma = 0.07$

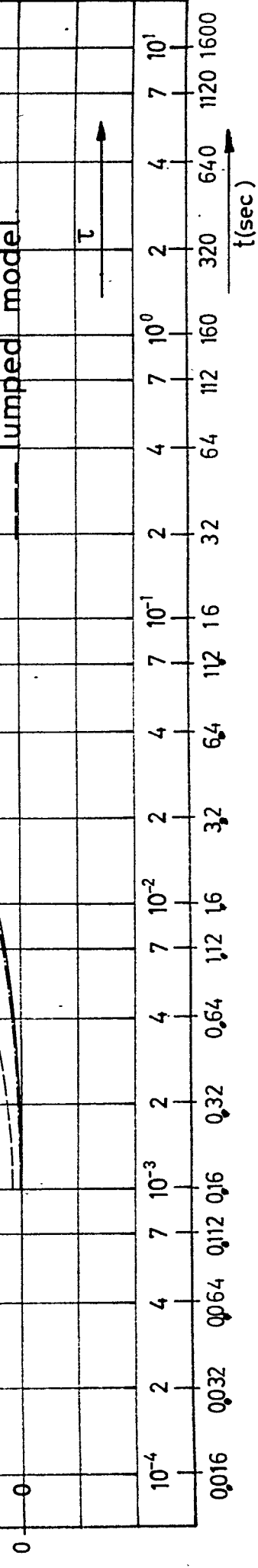
Response of the average fuel temperature, T_{av} ,
to a power step. Initial power = 20 MW

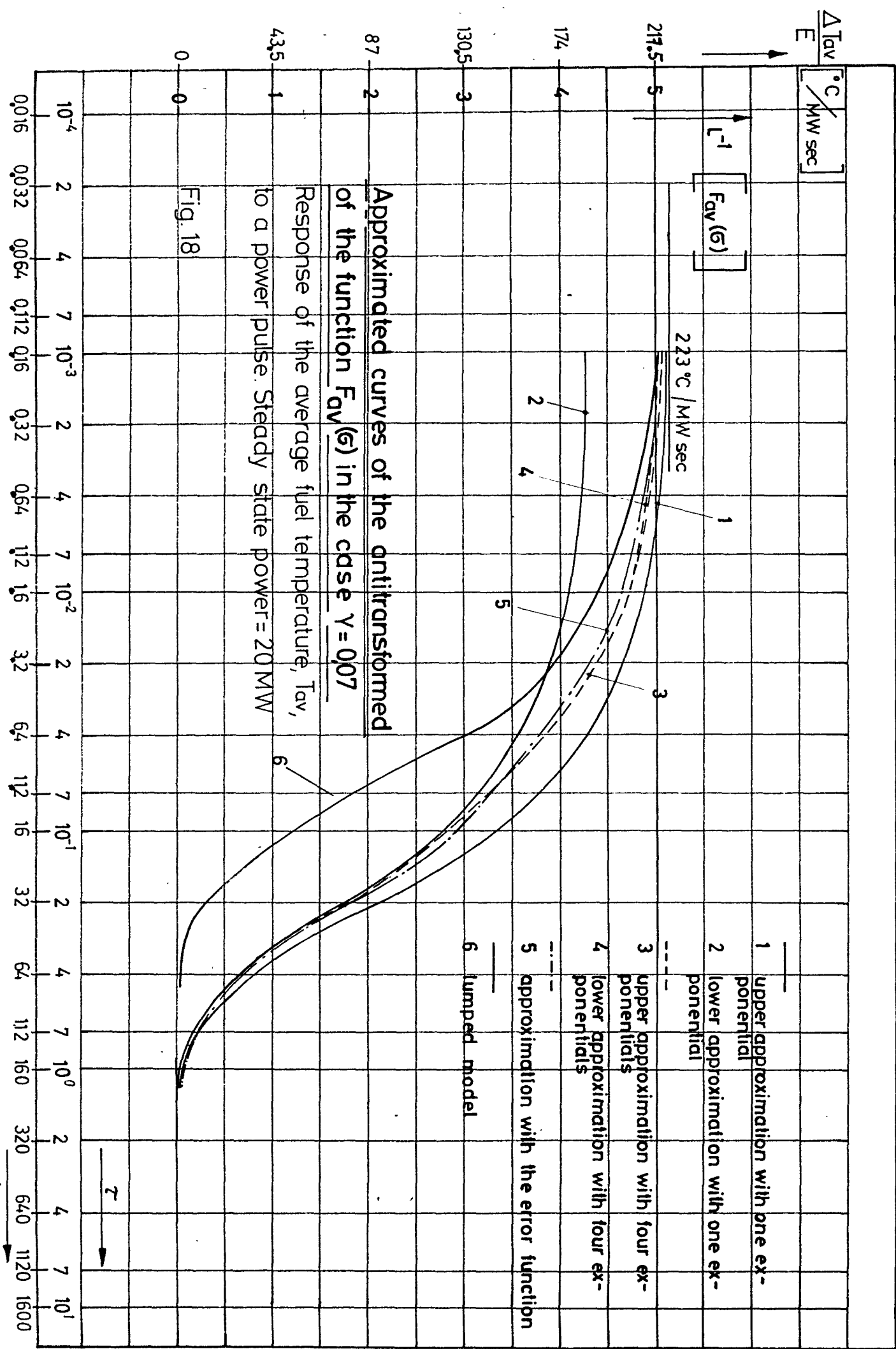
$$21.75 - 0.5$$

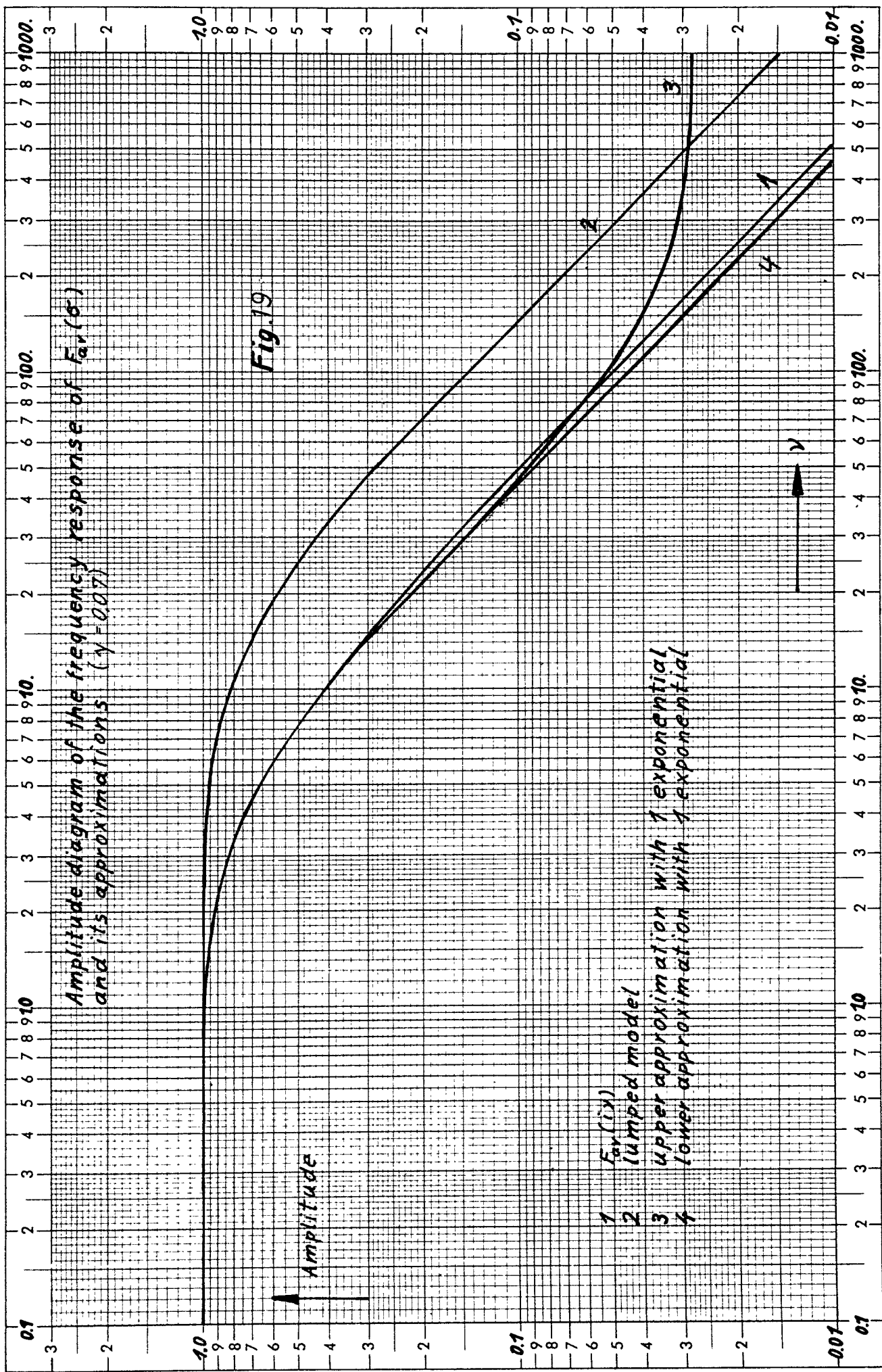
- 1 lower approximation.
 2 upper approximation.

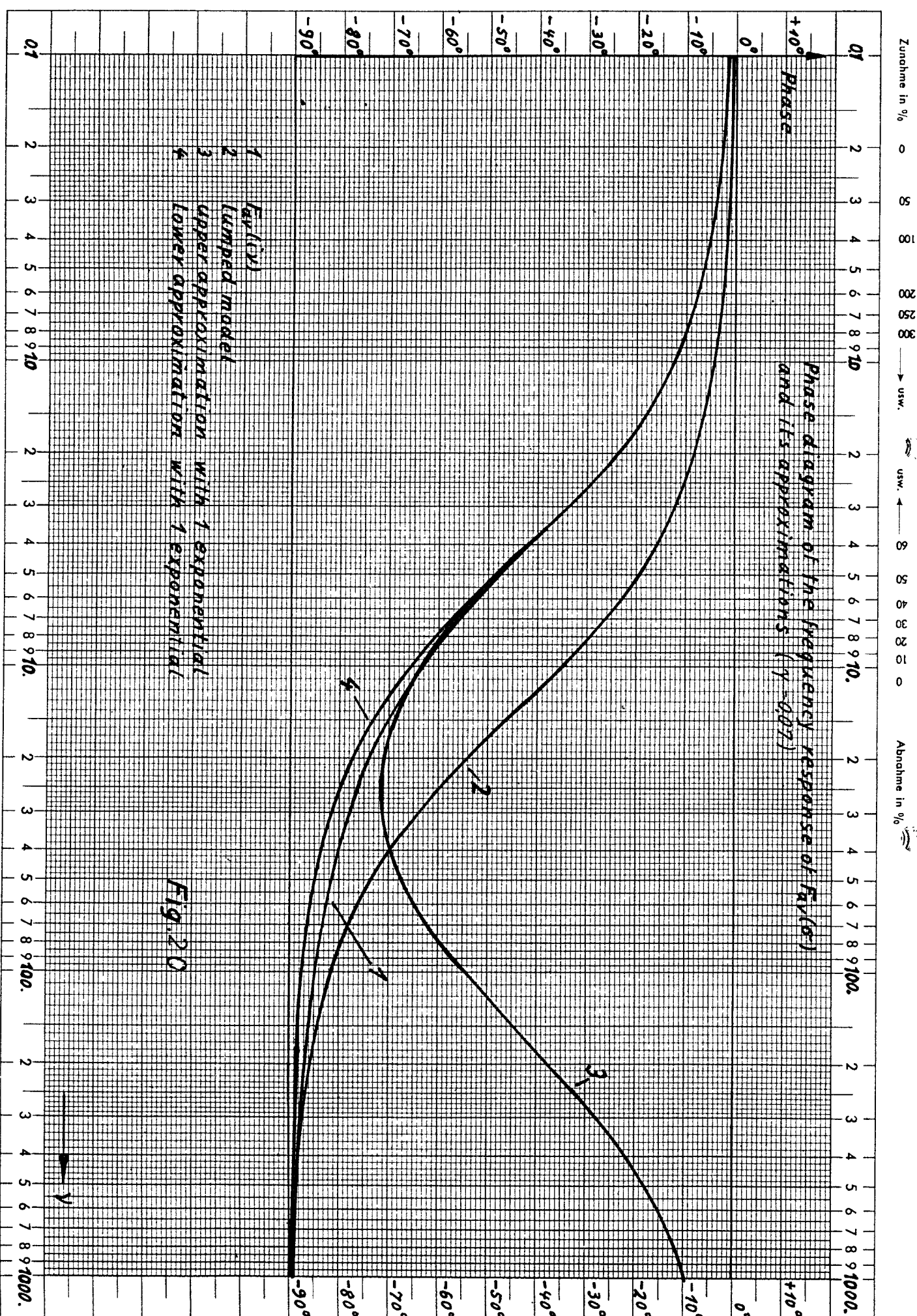
Fig. 17

- approximation with one
 exponential
 error function
 2 upper approximation.
 lumped model.

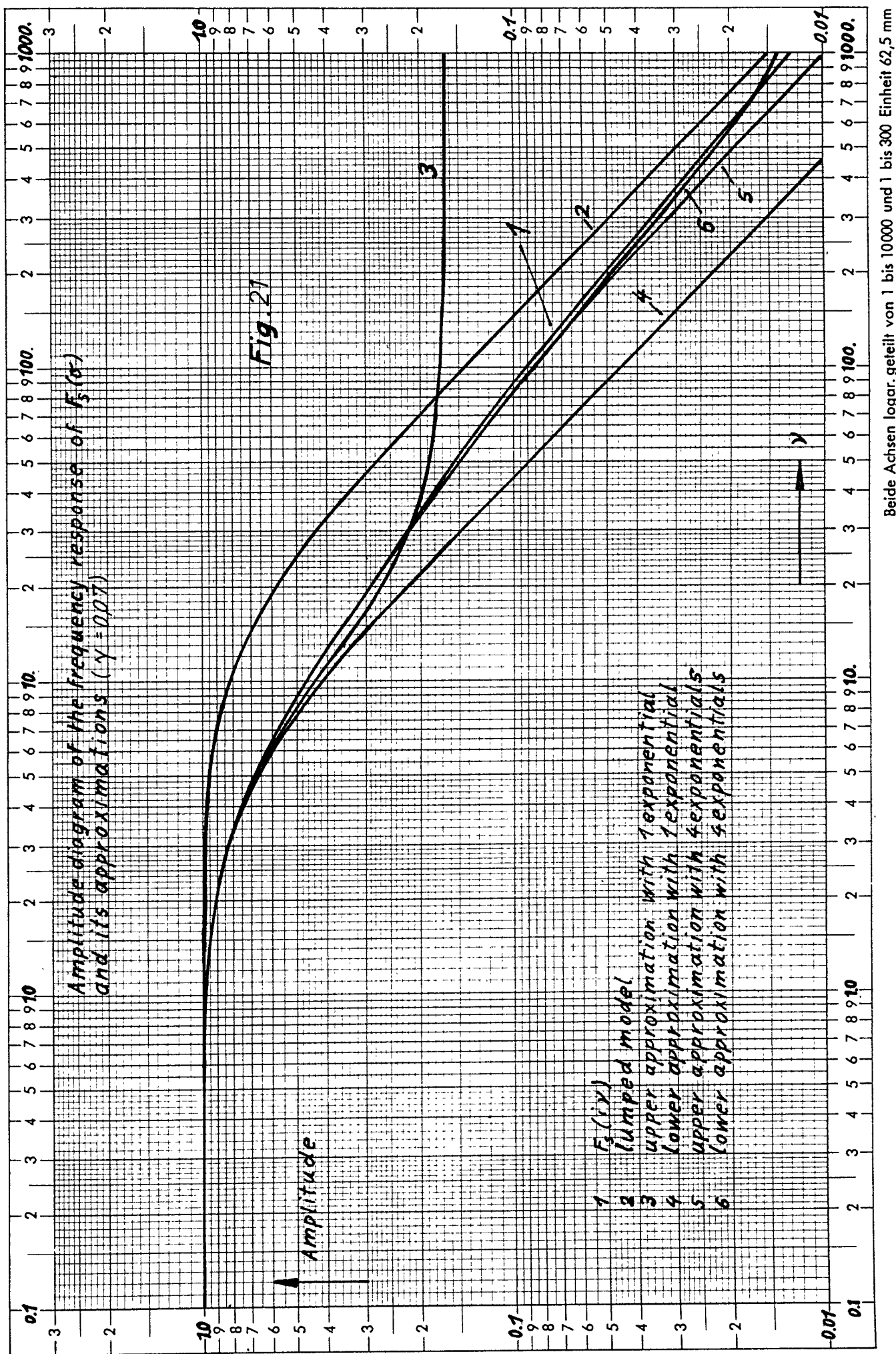






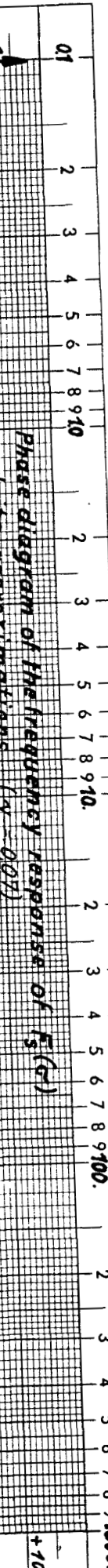


卷之三



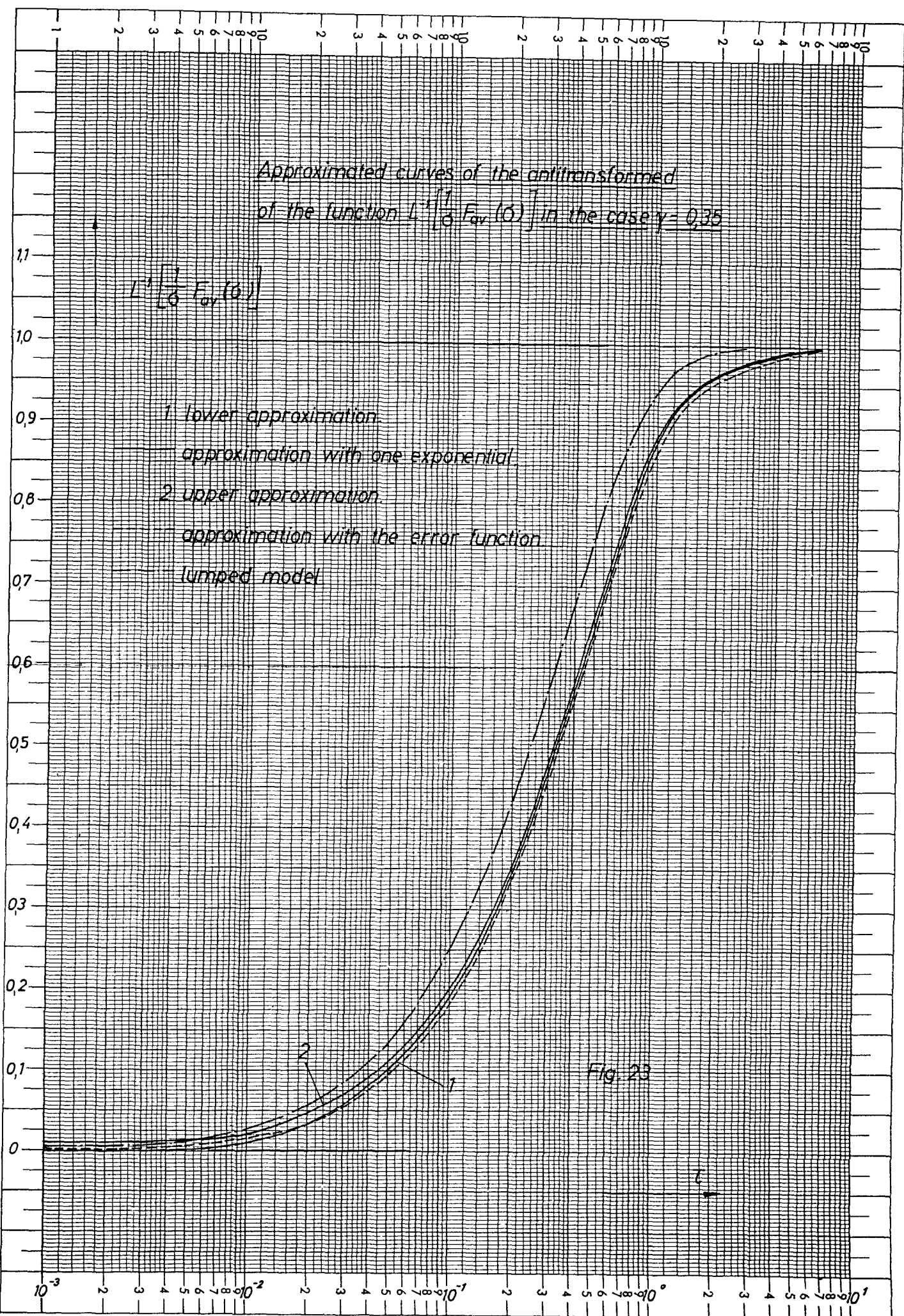
Zunahme in % 0 5 8 10 15 20 25 30 35 40 usw. usw. ← 8 8 8 8 8 8 8 8 8 8 0

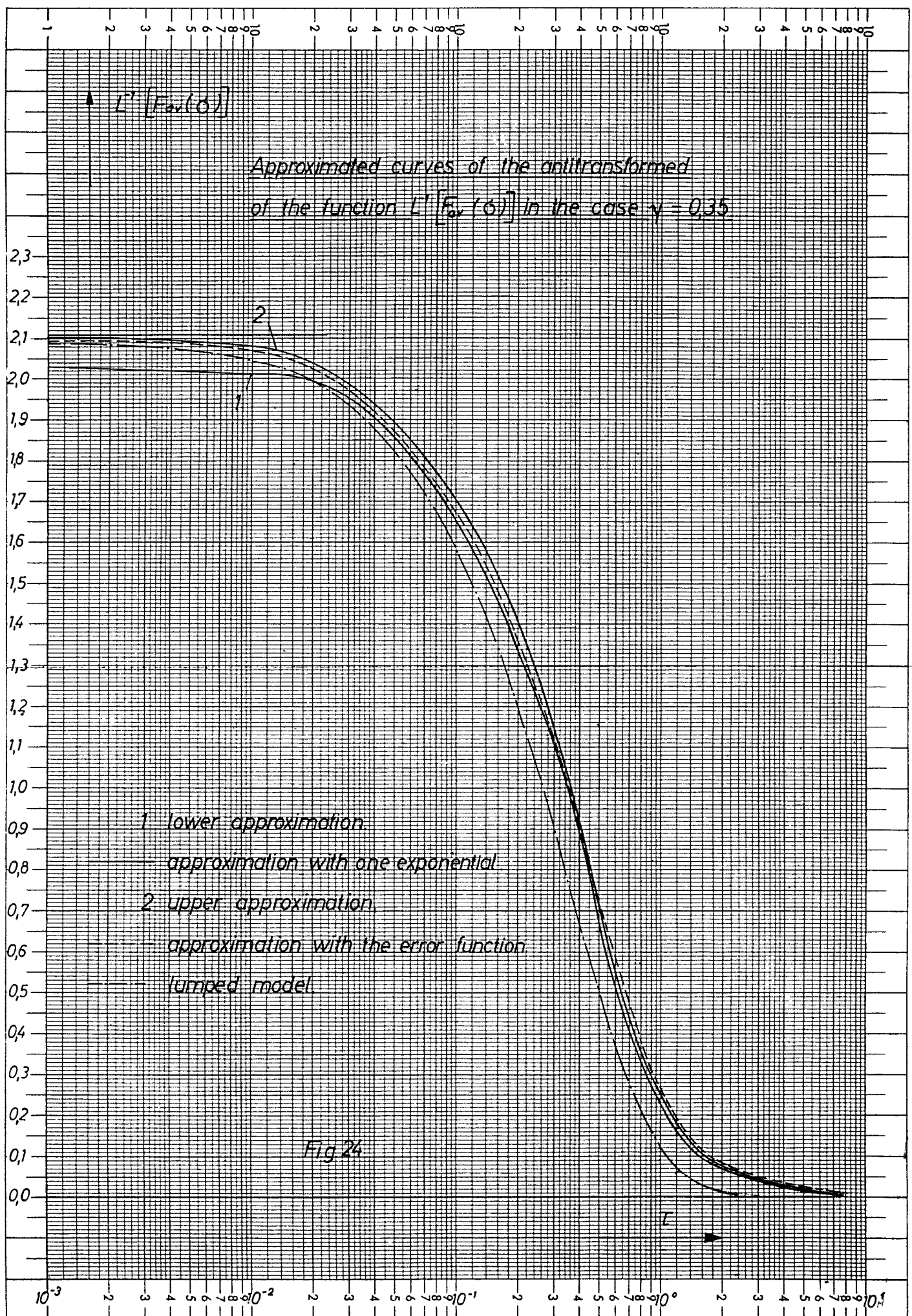
Abnahme in % 2 3 4 5 6 7 8 9 10. 2 3 4 5 6 7 8 9 10. 2 3 4 5 6 7 8 9 10. 2 3 4 5 6 7 8 9 10. 2 3 4 5 6 7 8 9 10.



- 1 $F_3(s)$
- 2 lumped model
- 3 upper approximation with 1 exponential
- 4 lower approximation with 1 exponential
- 5 upper approximation with 2 exponentials
- 6 lower approximation with 2 exponentials

Fig. 22





1.2 $\downarrow L^{-1} \left[\frac{1}{\sigma} F_{av}(\sigma) \right]$
 of the function $\frac{1}{\sigma} F_{av}(\sigma)$ in the case $\gamma = 0,01$

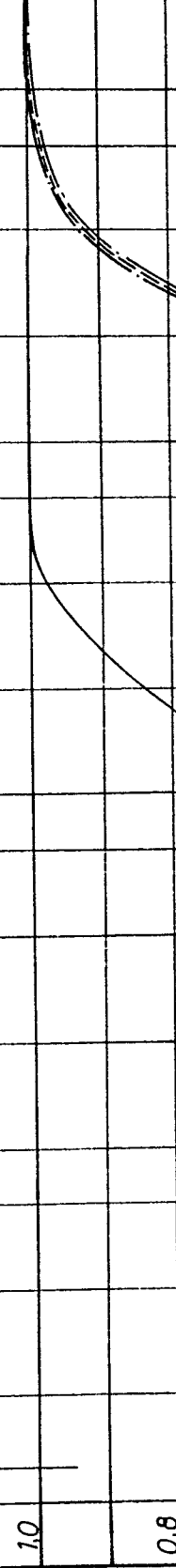
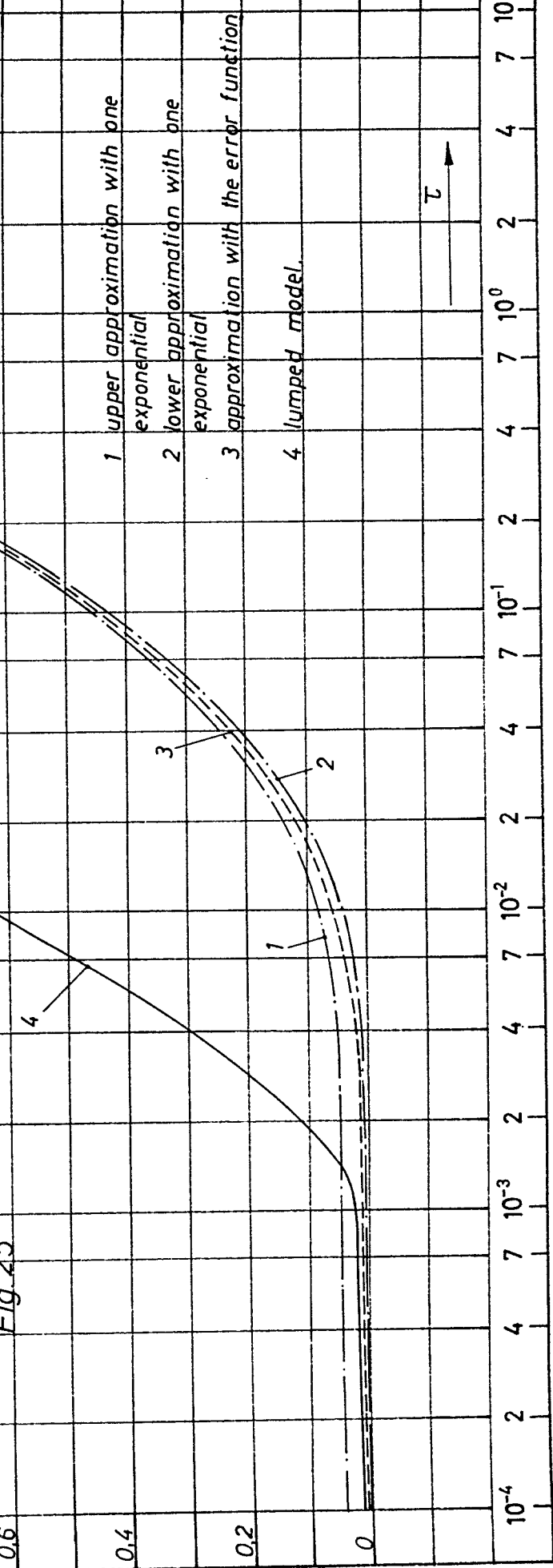


Fig. 25



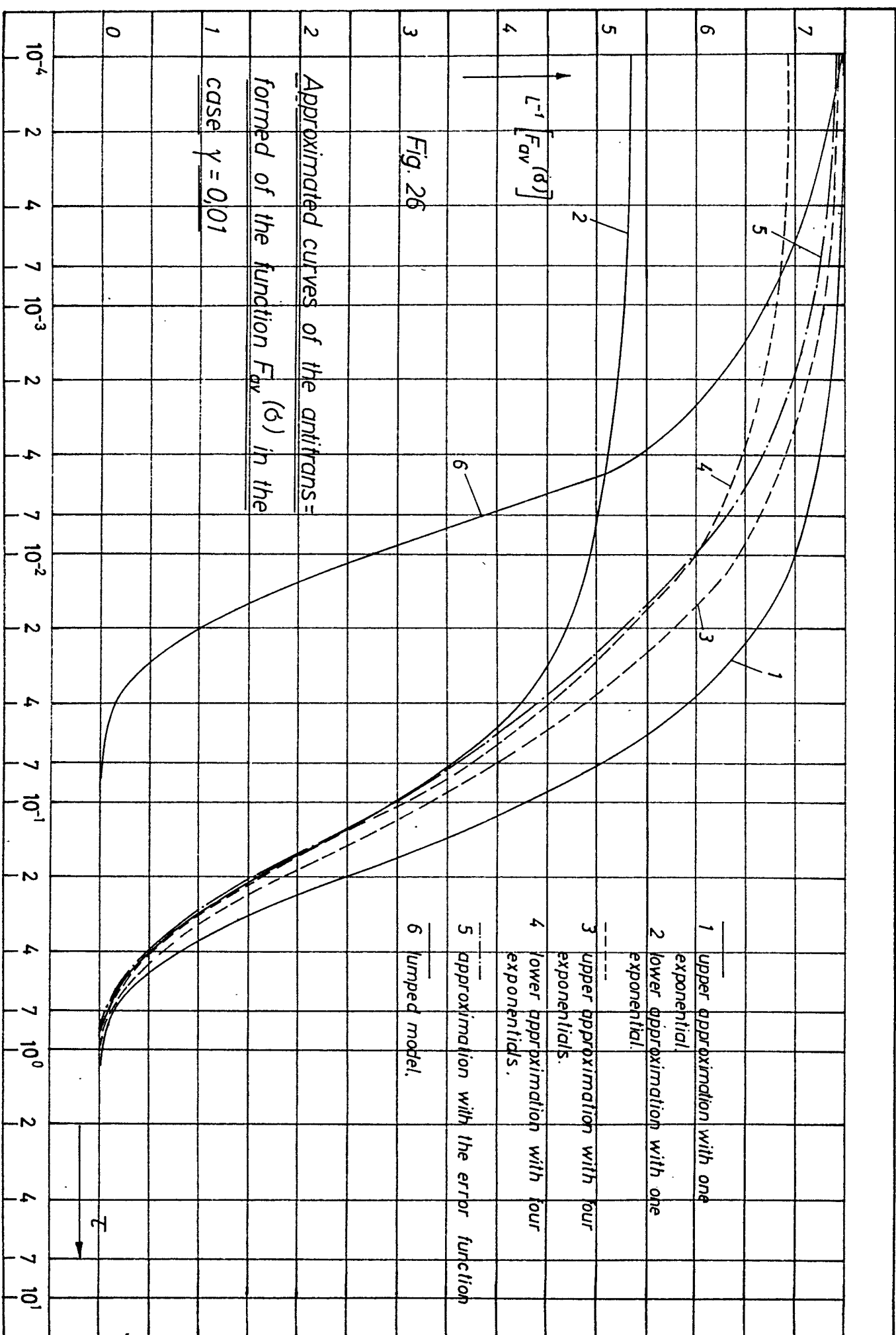
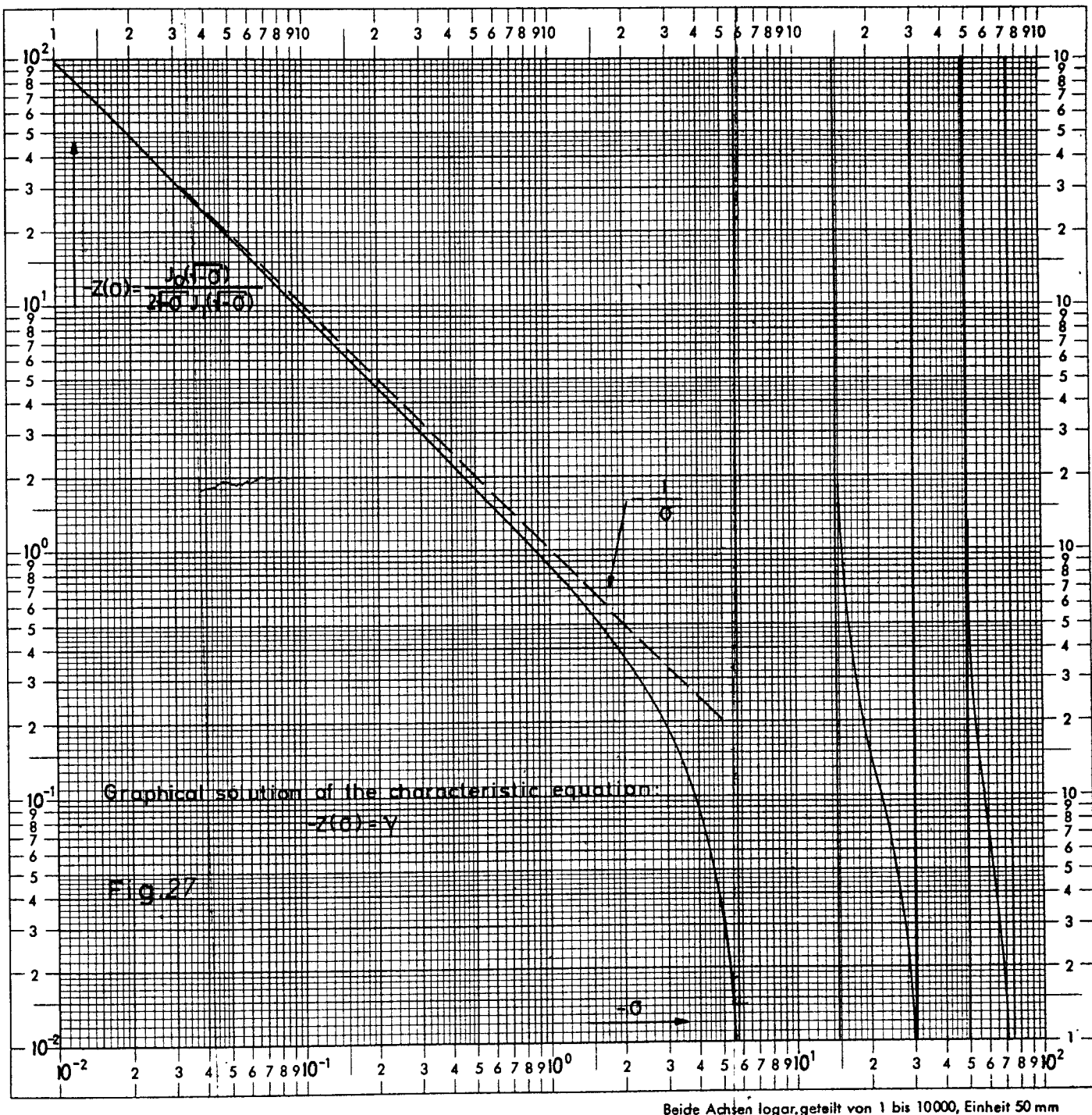


Fig. 26

2 Approximated curves of the antitransformation of the function $F_{\alpha}^{-1}(s)$ in the case $\gamma = 0,01$



T a b l e 1

Relationship between the zeros " σ_n " and the normalized zeros " $\bar{\sigma}_n$ " of
the characteristic equation

$$\boxed{\sigma_n = b_n + (a_n - b_n) \bar{\sigma}_n}$$

$\sqrt{a_n}$ = n-th zero of the Bessel function J_0

$\sqrt{b_n}$ = n-th zero of the Bessel function J_1

n	a_n	b_n
1	5.783062	0
2	30.471504	14.681925
3	74.886523	49.218643
4	139.03947	103.50010
5	222.93177	177.52093
6	326.56465	271.28066
7	449.93197	384.78353
8	593.04425	518.02215
9	755.89254	671.00167
10	938.47872	843.71659
11	1140.8046	1036.1767
12	1362.8722	1248.3714
13	1604.6754	1480.3102
14	1866.2227	1731.9830
15	2147.5068	2003.3949
16	2449.5277	2294.5537
17	2769.2959	2605.4389
18	3109.7909	2936.0792
19	3470.0346	3286.4422
20	3850.0163	3656.5604